CAPITAL UNIVERSITY OF SCIENCE AND TECHNOLOGY, ISLAMABAD

Design and Characterization of pH-Responsive Polymeric Networks: A Promising Approach for Enhanced Bioavailability and Controlled Drug Delivery of Ticagrelor

by

Alina Javaid

A thesis submitted in partial fulfillment for the degree of Master of Philosophy

in the

Faculty of Pharmacy
Department of Pharmaceutics

2025

Copyright © 2025 by Alina Javaid

All rights reserved. No part of this thesis may be reproduced, distributed, or transmitted in any form or by any means, including photocopying, recording, or other electronic or mechanical methods, by any information storage and retrieval system without the prior written permission of the author.

I dedicate this thesis to my loving and supportive family and friends, whose unwavering support has been crucial in helping me achieve my life goals.

CERTIFICATE OF APPROVAL

Design and Characterization of pH-Responsive Polymeric Networks: A Promising Approach for Enhanced Bioavailability and Controlled Drug Delivery of Ticagrelor

by

Alina Javaid

(MPH233020)

THESIS EXAMINING COMMITTEE

S. No.	Examiner	Name	Organization
(a)	External Examiner	Dr. Muhammad Iqbal Nasiri	HU, Islamabad
(b)	Internal Examiner	Dr. Muhammad Saalim	CUST, Islamabad
(c)	Supervisor	Dr. Nadia Shamshad Malik	CUST, Islamabad

Dr. Nadia Shamshad Malik
Thesis Supervisor
October, 2025

Dr. Nadia Shamshad Malik
Head
Department of Pharmaceutics
October, 2025

Dr. Muzaffar Abbas
Dean
Faculty of Pharmacy
October, 2025

Author's Declaration

I, **Alina Javaid** hereby state that my MS thesis titled "**Design and Characterization of pH-Responsive Polymeric Networks: A Promising Approach for Enhanced Bioavailability and Controlled Drug Delivery of Ticagrelor**" is my own work and has not been submitted previously by me for taking any degree from Capital University of Science and Technology, Islamabad or anywhere else in the country/abroad.

At any time if my statement is found to be incorrect even after my graduation, the University has the right to withdraw my MPhil Degree.

(Alina Javaid)

Registration No: MPH233020

Plagiarism Undertaking

I solemnly declare that research work presented in this thesis titled "**Design and Characterization of pH-Responsive Polymeric Networks: A Promising Approach for Enhanced Bioavailability and Controlled Drug Delivery of Ticagrelor**" is solely my research work with no significant contribution from any other person. Small contribution/help wherever taken has been duly acknowledged and that complete thesis has been written by me.

I understand the zero tolerance policy of the HEC and Capital University of Science and Technology towards plagiarism. Therefore, I as an author of the above titled thesis declare that no portion of my thesis has been plagiarized and any material used as reference is properly referred/cited.

I undertake that if I am found guilty of any formal plagiarism in the above titled thesis even after award of MPhil Degree, the University reserves the right to withdraw/revoke my MPhil degree and that HEC and the University have the right to publish my name on the HEC/University website on which names of students are placed who submitted plagiarized work.

(Alina Javaid)

Registration No: MPH233020

Acknowledgement

In the name of Allah, the most gracious and the most merciful; and prayers and peace be upon Muhammad, His servant and messenger. First and foremost, I would like to acknowledge my limitless thanks to Allah Almighty and to his last Prophet Muhammad (S.A.W) without their guidance this work would have never become completed. I owe a deep depth of gratitude to our University, Capital University of Science & Technology (CUST) for giving me such an opportunity to complete this work. A special thanks to the Dean Dr. Muzaffar Abbas for encouraging throughout the entire process.

I would like to acknowledge and very grateful to my Supervisor Dr. Nadia Shamshad Malik who has been always generous during all phases of the research and for all the valuable lessons that I learned during this period, I thank her from the bottom of my heart.

My thanks and appreciation also goes to my friend Noor ul ain. Last but not least, I want to express my wholehearted thanks to my family specially my parents, and brothers who have provided me generous support throughout my life and specially in doing my research. Because of their unconditional love, support and prayers, I have completed this thesis.

(Alina Javaid)

Abstract

A pH-responsive interpenetrating polymer network (IPN) hydrogel was engineered using xanthan gum (XG), carboxymethylcellulose (CMC), and acrylic acid (AA) crosslinked with N, N′-methylenebisacrylamide (MBA) to enhance oral delivery of ticagrelor (TGR)-a BCS Class IV antiplatelet drug with low solubility (10–15 μg/mL) and bioavailability (≈36%). The optimized formulation (F5) achieved 90.4 ± 0.52% drug entrapment efficiency and exhibited pH-triggered swelling, demonstrating a 2.41-fold higher equilibrium swelling ratio at pH 6.8 (13.02 ± 0.41) versus pH 1.2 (5.41 ± 0.32; $p < 0.001$). In vitro release studies revealed pH-dependent sustained release: 86.83% cumulative drug release at pH 6.8 over 24 h compared to 47.85% at pH 1.2 ($p < 0.001$). Release kinetics followed anomalous (non-Fickian) diffusion (Korsmeyer–Peppas model; $R^2 > 0.91$, $n = 0.47$–0.59), indicating coupled diffusion/polymer relaxation. Physicochemical characterization (FTIR, DSC/TGA, PXRD, SEM) confirmed covalent crosslinking, thermal stability (degradation onset $>200^oC$), amorphous drug dispersion, and a porous microstructure. Acute oral toxicity studies (OECD 423; mice (Balb/c), 2 g/kg) showed no significant alterations in hematological/biochemical parameters ($p > 0.05$) or histopathology, affirming safety. This engineered IPN hydrogel effectively addresses the critical solubility and bioavailability limitations of ticagrelor through pH-triggered swelling and sustained release, while demonstrating excellent safety in acute toxicity studies, presenting a highly promising strategy for enhancing its oral therapeutic efficacy in acute coronary syndrome.

Contents

List of Figures

List of Tables

Abbreviations

AA	Acrylic acid
ACS	Acute coronary syndrome
ADP	Adenosine diphosphate
AMPS	2-Acrylamido-2-methylpropane Sulfonic Acid
ANOVA	One-way analysis of variance
APS	Ammonium persulfate
β-CD	Beta-Cyclodextrin
CDDS	Controlled drug delivery systems
CMC	Carboxymethyl cellulose
DSC	Differential scanning calorimetry
EE	Entrapment Efficiency
FTIR	Fourier transform infrared
HPMC	Hydroxypropyl Methylcellulose
HPβCD	Hydroxypropyl Beta-Cyclodextrin
MBA N	N′-methylene bisacrylamide
NSTE	Non–ST-segment elevation
NSTEMI	Non-ST-segment elevation myocardial infarction
PEG	Polyethylene Glycol
PLATO	Platelet Inhibition and Patient Outcomes
PLGA	Poly(lactic-co-glycolic acid)
PVA	Polyvinyl Alcohol
PVP	Polyvinylpyrrolidone
PXRD	Powder X-ray diffraction
SEM	Scanning electron microscopy

SGF	Simulated gastric fluid
SIF	Simulated intestinal fluid
TGA	Thermo-gravimetric analysis
XG	Xanthan gum

Chapter 1

Introduction

1.1 Background

Cardiovascular diseases (CVDs) are the leading cause of deaths worldwide, causing an estimated 17.9 million deaths annualy, with acute coronary syndrome (ACS) playing significant roles in this concerning number [1]. Regardless of the recent advances and improvement in pharmacological interventions and more extensive adoption of interventional strategies, the incidence of ACS appears to be notably high especially in low- and middle-income areas of the world, including Southeast Asian ones, as evidenced by the 30% increase in the number of people hospitalized due to ACS over the last three years alone, which testifies to the inability to fully address the problem on a therapeutic level and management in patient care [2]. Ticagrelor (TGR) is a new antiplatelet agent. It is a non-competitive antagonist which binds on PY12 receptor in a reversible manner. TGR is used as a prescription drug in ACS to reduce the chances of myocardial infarction, stroke and cardiovascular death. TGR exhibits BCS class IV characteristics with an aqueous solubility measuring at 10-15 μg/mL and permeability rate that generates an oral bioavailability of ≈36%. The reduced dissolution rate of the drug leads to decreased bioavailability, making it one of its primary challenges [3]. The design of an effective drug delivery system which improves the dissolution of TGR represents a key requirement to obtain efficient Acute Coronary Syndrome therapy.

The development of polymeric networks has led to one of the promising delivery systems due to their s mall size, hydrophilicity, ability to swell, high efficiency in trapping drugs, stability, biocompatibility, and cost-effective manufacturing. Polymeric networks such as hydrogels encapsulate both hydrophilic and lipophilic drugs. They are created using natural or synthetic building blocks such as monomers, polymers, or their combinations [4]. Hydrogels that respond to stimuli are termed as smart biomaterials, and drug release can be initiated by external stimuli such as pH, temperature, electrical and magnetic fields, light, and concentration of the biomolecules [5].

Hydrogels have found application in several biomedical and pharmaceutical applications. Hydrogels compared to other synthetic biomaterials closely mimic the physical properties of living tissues due to their relatively high water content and their soft and rubbery texture. Hydrogels exhibit little affinity to absorb body fluids proteins due to their low interfacial tension. Moreover, since the molecules of various sizes can diffusion into (drug loading) and out of (drug release) hydrogels, it becomes feasible to utilize dry or swollen polymeric networks as drug delivery vehicles in oral, nasal, buccal, rectal, vaginal, ocular and parenteral applications [6].

Biopolymers consist of biomolecules that are joined together by covalent bonds between their repeating units. There are many uses for biopolymers in different industries, including water pollution, sensing, tissue engineering, catalysis and drug carrier [7]. Moreover, biopolymers, owing to being non-toxic, having high levels of biocompatibility and biodegradability and sensitivity to the environment, may have useful applications in the pharmaceutical sector [8]. Smart carriers for controlled drug, peptide and protein release have been made using biopolymers such as starch and their derivatives, carboxymethyl cellulose and their derivatives [7], carrageenan [9], and chitosan [10].

The development of controlled drug delivery systems (CDDS) aims to address the issues inherent in conventional drug delivery. By releasing a specific dose of the medicine at each time point for a predetermined amount of time, CDDS maintains drug plasma levels constantly. This enhances patient compliance and

lowers the dosage and frequency of medicine. Reduced exposure to the biological environment lowers the toxicity and side effects of drugs [11].

Xanthan gum (XG) is a natural, anionic polysaccharide with wide pharmaceutical applications. XG polymeric networks have been used as drug carriers for the administration of numerous drugs. Its hydrophilic matrix prolongs residence time in the gastrointestinal tract, providing controlled drug release [12].

It exhibits high stability at low pH, which ensures that the drug is not degraded in the stomach and that the drug is released in an alkaline environment. XG is naturally mucoadhesive, a property which increases the duration of retention of the drug and its therapeutic effect [13].

As a result, this polymer has been thoroughly investigated for a wide range of pharmaceutical and biological applications in recent years. In this regard, a range of formulations based on xanthan gum showed encouraging outcomes for several applications, such as hydrogels for the administration of different medications, transdermal patches [14], vaginal delivery [15], anticancer drugs [16], controlled-release tablets [17], and periodontal diseases [18].

Carboxymethyl cellulose (CMC) is a biodegradable and easily available derivative of cellulose. Drug delivery systems could benefit greatly from CMC usage in their development process based on its physicochemical qualities, biocompatibility, biodegradability, and low immunogenicity. CMC can absorb large amounts of water and swell to form polymeric networks with desired properties when cross-linked with an appropriate polymer or monomer [19].

CMC is highly hydrophilic because it contains numerous carboxyl (-COOH) and hydroxyl (-OH) groups. CMC has received increased attention in hydrogel preparation because of its excellent properties, such as, water-solubility, more biocompatible, high swelling ability, abundance, and affordability [20].

Acrylic acid (AA) is strongly bioadhesive, pH-sensitive, and also mechanically robust, which makes it a perfect monomer to fabricate polymeric networks displaying pH-sensitive behavior [21]. AA is a monomer crosslinked to create polymeric

networks with high water-absorbing capacity [22]. The polyacrylic acid (PAA) -based polymeric networks swell significantly at basic pH due to the ionization of the carboxylic acid (CA), as its pKa value ranges from 4.5–5 [23].

1.2 Problem Statement

TGR is a potent antiplatelet drug, however, its efficacy is significantly reduced due to poor bioavailability, thereby, there is a compromise of the antiplatelet effect, vital in critical cases. Moreover, conventional immediate-release dosage forms of TGR require twice daily dosing, which can impact the patient compliance and adherence to the regimen, fluctuations of the plasma concentrations, and thus increasing the risk of bleeding. The study aims to develop an advanced delivery system to improve the bioavailability and provide a controlled release that can help minimize the dosing frequency, improving therapeutic outcomes, and patient compliance.

1.3 Study Gap

To our knowledge, this is the first report on the development of xanthan gum, carboxymethyl cellulose and acrylic acid based interpenetrating polymeric network (IPN) hydrogel system developed as an oral delivery system of TGR. The novelty of the combination of these polymers into IPN framework provides a novel, biocompatible and pH-sensitive system that can increase the bioavailability of TGR, minimize dosing regimen and improve therapeutic outcome in the management of ACS. The fabricated IPN hydrogels in this work were characterized systematically with respect to their physicochemical characterization, swelling kinetics, pH-responsive behavior, in vitro drug release profile and applicability to oral TGR delivery system. The results of the research will have potential impact on the area of stimuli-responsive drug delivery systems and present a practical contribution to the field, which can help to improve the therapeutic effectiveness of poorly bioavailable cardiovascular drugs.

1.4 Aims and Objectives

1. To design and optimize pH-sensitive hydrogels for the controlled delivery of Ticagrelor (TGR) using natural polymers—carboxymethyl cellulose (CMC) and xanthan gum (XG)—in combination with the monomer acrylic acid (AA), to enhance the dissolution rate and oral bioavailability of TGR.

2. To evaluate the pH-responsive swelling behavior and in vitro drug release kinetics of the synthesized hydrogels under simulated gastrointestinal (GI) conditions.

3. To characterize the physicochemical properties of the hydrogels using analytical techniques, including Fourier-transform infrared spectroscopy (FTIR), scanning electron microscopy (SEM), differential scanning calorimetry (DSC), thermogravimetric analysis (TGA), and X-ray diffraction (XRD).

4. To assess the acute oral toxicity and biocompatibility of the TGR-loaded hydrogels through in vivo studies, ensuring their safety for oral administration.

Chapter 2

Literature Review

2.1 Acute Coronary Syndrome

Acute coronary syndrome (ACS), a form of ischemic heart disease, is used to describe a group of conditions that are related to the acute (sudden) decrease in blood flow to the heart. There are two broad forms of acute coronary syndrome: non–ST-segment elevation (NSTE) ACS and ST-segment elevation myocardial infarction (STEMI). NSTE ACS may be beyond classified into unstable angina or non-ST-segment elevation myocardial infarction (NSTEMI) [24].

ACS is one of the primary causes of mortality, illness, and lost productivity. The major pathological mechanism responsible for both unstable angina and myocardial infarction is the rupture of atherosclerotic plaques, subsequently causing coronary thrombosis. Platelets attach to ruptured plaques, accumulate, and produce secondary messengers that trigger further vasoconstriction and thrombosis. They also act as a surface for the clotting cascade to be activated. Antiplatelet medications have thereby contributed significantly to the management of acute coronary syndromes and the prevention of recurrent episodes [25]. The European Society of Cardiology recommends antithrombotic medication administration as a key pharmacotherapy component for ACS patients [26]. Antiplatelet medication is

an essential component of the medical regimen during the acute phase of acute coronary syndromes, as well as secondary prevention after stabilization [27].

2.2 Ticagrelor

TGR is a new generation of antiplatelet agent, cyclopentyl-triazolo-pyrimidine. It is recommended to decrease the occurrence of myocardial infarction, stroke, and cardiovascular mortality in individuals with ACS [28].

It is a non-thienopyridine drug. Astra Zeneca first discovered the drug and it was given approval in 2011 by the FDA. The compound is described as a nucleoside analog since its side chains include difluorophenyl cyclopropyl, propyl-thiol and hydroxyethoxy cyclopentane-1,2-diol, as shown in Figure 2.1 [29].

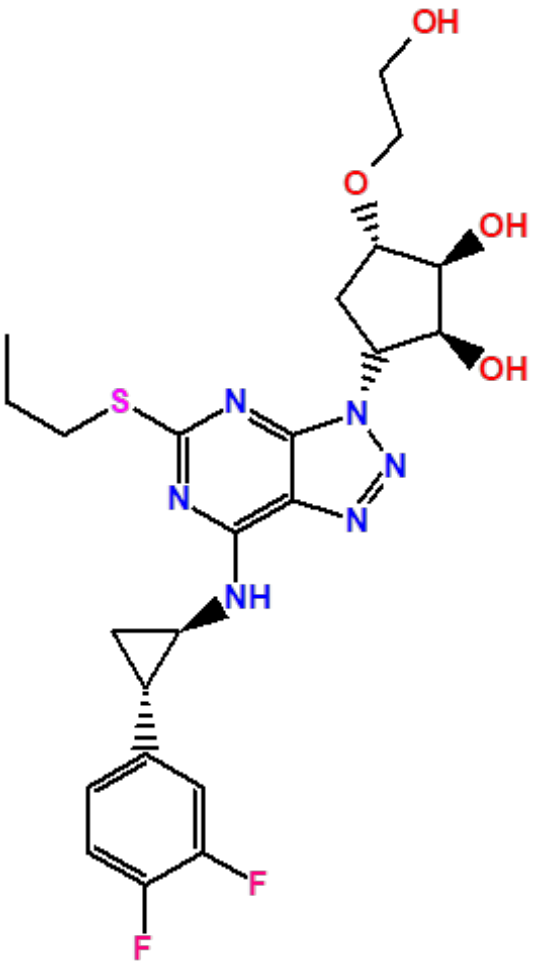

FIGURE 2.1: Structure of TGR.

2.2.1 Mechanism of Action

TGR is orally administered direct-acting $P2Y_{12}$-receptor antagonist. In vitro research indicates that TGR binds to a different site on the $P2Y_{12}$ receptor compared to the natural agonist adenosine diphosphate (ADP) in a reversible and noncompetitive manner [30].

Moreover, TGR exhibits characteristics of an inverse agonist. This indicates that with continued therapy, basal Gi-coupled signaling diminishes despite the absence of ADP stimulation [31].

2.2.2 Physicochemical Properties

TGR ($C_{23}H_{28}F_2N_6O_6S$) is a crystalline powder with a molecular weight of 522.6 g/mol [32]. Its water solubility of 10 μg/ml [33]. TGR shows no pKa value within the physiological range and is classified as a class IV medication (poor solubility, low permeability). There is no pH-dependent solubility of TGR. Its melting point is between 140^{o}C and 142^{o}C. TGR's partition coefficient has a log P (octanol/water) >4.0 [34].

2.2.3 Pharmacokinetics

TGR demonstrates rapid absorption, with peak plasma concentration (tmax) achieved within 1-2 hours' post-administration. This active drug obviates the need for hepatic transformation upon entering the systemic circulation. In healthy subjects, the mean half-lives of TGR and its active metabolite are reported to be 7.1-8.5 hours and 8.5-10.1 hours, respectively [35].

While renal excretion plays a role, the primary routes for the elimination of TGR and its metabolites are biliary and intestinal. According to a regional absorption study conducted on healthy volunteers, the absorption of TGR decreased as the dose moved further down the gastrointestinal tract [28].

2.2.4 Side Effects

TGR is mostly well - tolerated and the incidence of side effects is similar to that of clopidogrel. The unwanted effects of TGR are; bleeding more readily than usual - nosebleeds, bruising or bleeding that is slower to stop, sudden shortness of breath during resting - this may occasionally occur within the first few weeks of using TGR and is often mild, pains and swelling of your joints - these may be symptoms of gout (this is due to the fact that TGR may cause excessive uric acid in your blood), dizziness, indigestion, headaches, diarrhea, constipation and slight rash [36]. Moreover, dyspnea, cerebral hemorrhage, and early discontinuations due to adverse events are common with TGR. A dyspneic episode could lead to discontinuation of the treatment. In the PEGASUS-TIMI trial, 6.5% of patients taking 90 mg of TGR twice a day and 4.6% using 60 mg twice a day ceased their treatment due to dyspnea [37].

2.3 Dosing

According to American College of Cardiology (ACC)/American Heart Association (AHA) 2013 and the European Society of Cardiology (ESC) 2017 STEMI guidelines, TGR can be recommended as a first-line P2Y12 inhibitor with a 180 mg loading dose and 90 mg BD maintenance dosage. The plasma concentration of TGR at steady state during long term maintenance therapy at 60 mg and 90 mg BD is sufficient to produce high degrees of platelet aggregation inhibition in patients. The longer durations of platelet inhibition with TGR are achieved when the drug is administered BD compared to once daily (OD) [35].

2.4 Comparison with Other Anti-Platelets

It has been reported that patients receiving TGR have a more rapid onset of action compared to those taking clopidogrel. Additionally, TGR has shown positive results in patients' resistant to clopidogrel. Research also indicates that TGR is

more effective in preventing stroke, myocardial infarction, and vascular-related deaths in individuals with ACS, as well as in those with noncardioembolic, high-risk transient ischemic attack or non-severe ischemic stroke [37].

Compared to clopidogrel, a commonly used $P2Y_{12}$ inhibitor, TGR markedly lowers the rate of cardiovascular death owing to ACS according to the Platelet Inhibition and Patient Outcomes (PLATO) study [38]. TGR acts faster than clopidogrel and has more consistent and potent antiplatelet effects. The PLATO trial included 18624 patients with moderate to high risk of unstable angina, non-STEMI, or STEMI with planned primary percutaneous coronary intervention. Before attempting percutaneous coronary intervention, patients were randomized and treated immediately.

TGR reduced the primary outcome of cardiovascular mortality, myocardial infarction, and stroke by 16%. Irrespective of the type of stent, patient profile, or co-therapies administered, TGR decreased the risk of definitive stent thrombosis by around 33%. The advantages of TGR were compliant with conservative or invasive treatment approaches. TGR has a fast offset of antiplatelet effect versus prasugrel, thereby minimizing the chances of side effects like bleeding. Due to the mentioned reasons, TGR is now favored over other antiplatelets in clinical guidelines [30].

2.5 Hydrogels

Hydrogel is a polymer material with a structure that stores lots of water and biological fluids in its 3D framework. Due to biomimetic elements, hydrogels reveal outstanding flexibility, soft texture, superior ability to take up solutions when swollen, nontoxicity, biocompatibility and adjustable properties related to their mechanical strength [39]. A hydrogel is made by bonding together polymer chains with water molecules using simple reactions between monomers. Hydrogel is known as a material that cannot dissolve in water but can expand and contain a significant amount of water. For fifty years, hydrogels have stood out as promising

material for various applications. This flexibility is achieved through their similar water content in natural tissue [6]. Hydrogels are regarded as distinct in the field of biomedicine due to their unique features, compared to other nanomaterials. It is easy to inject hydrogels as liquid into the body since they set into a gel when exposed to body heat, and most are biocompatible. In addition, they support efficient movement of nutrition and products inside cells, and the water-based environment protects potentially harmful drugs and cells [40]. Hydrogels do not need expensive equipment and are simple to scale up, making hydrogels potential choices for commercial production. Hydrogels are mainly used in drug delivery as sustained-release, delayed-release, targeted release or stimuli-sensitive systems [41].

2.5.1 Hydrogel Preparation

Hydrogels can be prepared with different methods. A hydrogel is usually created by hydrolyzing and condensing specific precursors which leads to the formation of a solid, nanostructured network. Therefore, most studies are centered on making hydrogels through physical and chemical cross-linking, as shown in Figure 2.2. Chemically cross-linked hydrogels don't degrade while absorbing water, whereas physically cross-linked hydrogels dissolve and break down after prolonged exposure to fluid [42]. The methods of hydrogel preparation are illustrated in 2.2.

2.5.2 Physical Crosslinking

In physical crosslinking method, hydrogels are formed when a liquid turns into a gel due to variations in pH, temperature, mixing of different chemicals or ionic concentration are referred to as physical hydrogels, and are valued because no cross-linker was used [43]. Physical hydrogels are formed via hydrogen bonding, ionic interactions, block polymers, and protein interactions [44].

Hydrogen bonding cross-linking is a way of linking polymeric chains by forming hydrogen bonds which creates a nanostructured network [45]. In another method,

when blocks or grafts with amphiphilic properties are mixed in aqueous solutions, they assemble to form hydrogels or polymeric micelles, collecting the hydrophobic part of the polymer in a central core. In addition, crystallization can be used to create hydrogel networks based on block polymer materials [46].

In ionic interactions, the formation of hydrogel is promoted by ions which support the structure of the internal network. Usually, this method takes place at normal body temperature and pH. The produced hydrogels are not harmful, do not irritate the skin, stretch easily and have enough adhesion to be placed on the skin as a polymeric layer [47]. Protein interaction method involves genetically changed proteins or antigen - antibody reactions are used as the foundation for this cross-linking technique. This modification manipulates the arrangement of the peptides in hydrogels, permitting control over their properties [48].

2.5.3 Chemical Crosslinking

Chemical cross-linking involves the formation of covalent bonds, the presence of this linkage is irreversible. As a result of being cross-linked, these hydrogels have higher structural strength which makes them more attractive to researchers. The chemical crosslinking of hydrogels can be done using five major methods, as described in Figure 2.2 [49].

Enzymes are used instead of chemicals as reactants in enzymatic cross-linking, because they are less harmful. A lot of cross-linking experiments are carried out with biopolymers. Additionally, adding enzymes supports the linking of polymer chains in hydrogels [49]. Interaction between complementary chemical compounds involves secondary reactions are started in these hydrogels using different agents to help cross-link the hydrogel molecules. The group of these additives contains aldehydes and those that help promote condensation [50].

In energy with high levels of radiation, the development of cross-link bonds is promoted through the application of gamma radiation or electron beam. Studies have discovered a way to combine this cross-linking method and enzymes to develop hardening of hydrogels using macromolecules [51].

The fabrication of hydrogels with free-radical polymerization depends on utilizing hydrophilic polymers that might be synthetic, semi-synthetic or natural [52]. Some reactions are favored when enzymes are used as catalysts, while commonly, free radical initiators are used to start reactions by different means. Sources of radiation including temperature, ultraviolet, oxidation, microwaves and gamma rays have been used to initiate reactions resulting in free radicals [53]. Click reactions is used for cases when various heteroatom-linked molecules are formed using reactions that are rapid, spontaneous, versatile, extremely selective and don't result in secondarproducts with high yields and high efficiency in a variety of mild conditions. Multiple methods from click chemistry can be used to add features and shape hydrogels with desired qualities [54].

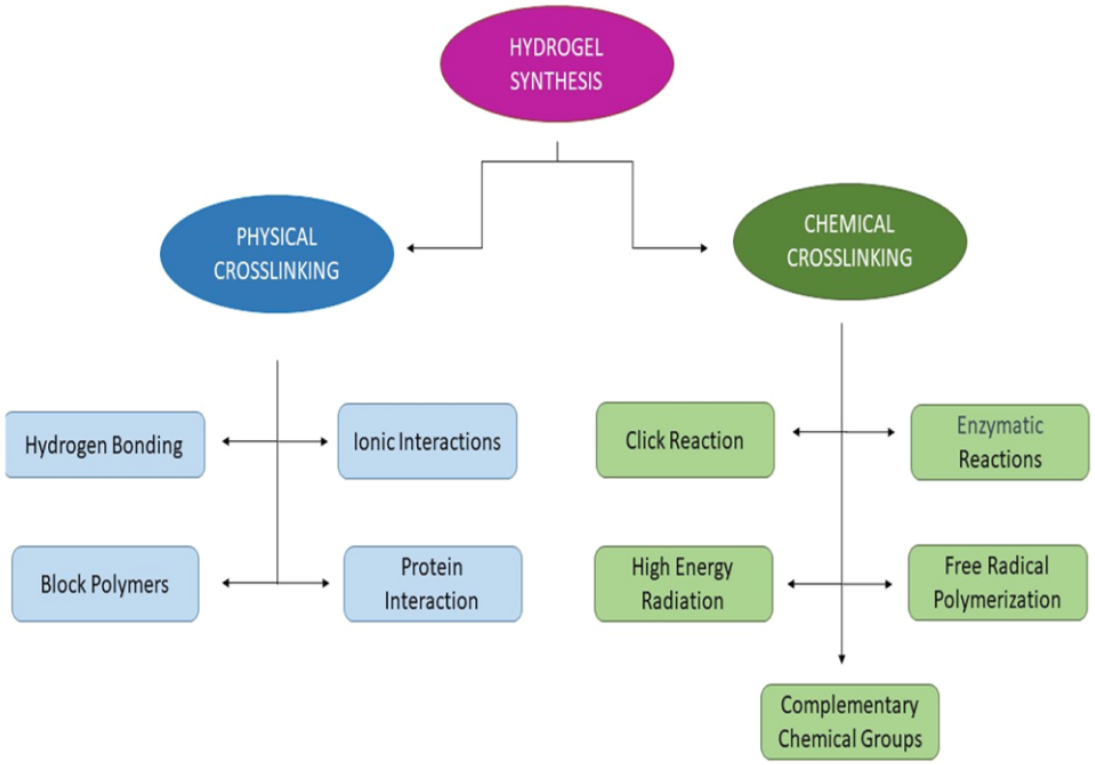

FIGURE 2.2: Schematic overview of methods of hydrogel synthesis.

2.6 pH - Responsive Hydrogels

A stimuli-responsive hydrogel is a 3D structure made of hydrophilic polymers which changes its shape or phase when exposed to environmental changes. The

functional groups that appear along the polymer chains often make hydrogels sensitive to their environment changes. pH responsive hydrogels showing pH-control swelling can be made swollen through ionic interactions. Acidic or basic pendant groups are found in the ionic networks. In situations of suitable pH and ionic concentration in water, the pendant groups in the gel are able to become charged. Electrostatic repulsion between the molecules allows for more uptake of solvent in the network [55].

The broad variance in pH between the stomach and the intestine which is typical in the GI tract, enables pH-responsive systems to deliver drugs only in the stomach. Differences in pH are noticed in both the vaginal tract, the gut, blood vessels, the space around cells and the skin [56]. In addition, changing pH values between regular and malignant cells is applied in medicine and gene delivery by using pH-sensitive hydrogels to target specific places in the body such as organs and in the treatment of cancer by destroying cancer cells [57]. pH-responsive drug delivery systems are created using just two fundamental approaches. The purpose of initiating the organ- or site-based approach is to elect polymers that have ionizable groups. When these ionizable groups react to changes in pH, they can release the drug in a controlled manner by altering their shape, their solubility or their size, as shown in Figure 2.3 [58].

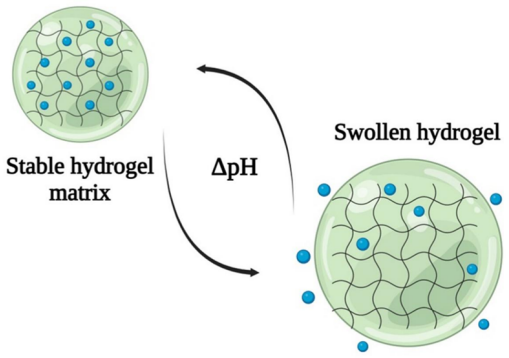

FIGURE 2.3: Swelling/deswelling of drug loaded hydrogel due to variation in pH [59].

Another method involves having ionic bonds form between the pH-sensitive polymer and the drug. A pH change can cause the ionic interaction to dissolve which

releases the drug from inside the polymer [60]. An example is the use of multi-responsive hydrogels based on poly(methacrylic acidco-N-vinylpyrrolidone) and a peptide crosslinker as drug carriers for oral insulin delivery. It was observed that insulin was not released at the stomach acid pH but was only release after the peptide crosslinker was degraded by the enzyme trypsin at higher pH [61].

The summary of the beneficial applications of pH responsive hydrogels in durg delivery system is illustrated in Figure 2.4.

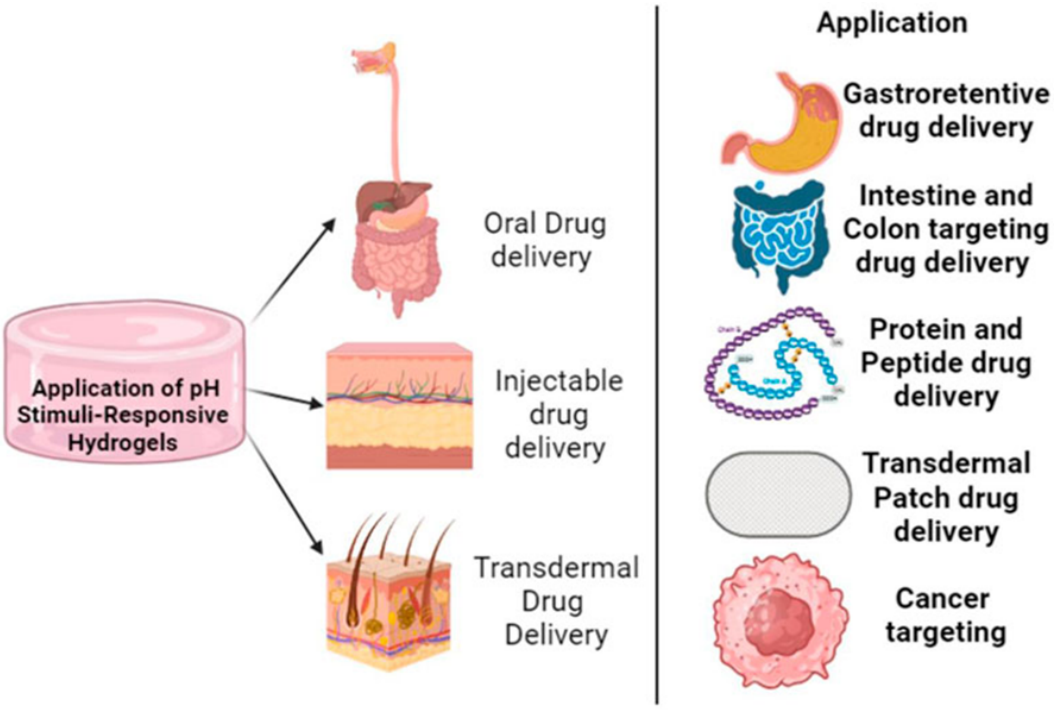

FIGURE 2.4: Applications of pH- responsive hydrogels in drug delivery [62].

2.7 Controlled Drug Delivery System

In CDDS, the drug remains at a steady amount in blood and tissues over a long period. A desired amount of drug is released from a CDDS at set intervals during a fixed time. As a result, patients get smaller and less frequent doses, improving their compliance. Reducing drug exposure to the body helps avoid harmful effects from drugs. The effectiveness of the medicine is increased by this dosage form [63]. The benefits of using CDDS is shown in Figure 2.5.

With conventional delivery systems there are the constraints of little synchronization between the time needed to achieve therapeutically effective plasma concentrations of the drug and the time profile of drug release that is displayed by the dosage form. Greater awareness of the concept of pharmacokinetics and disease symptom fluctuation due to diurnal rhythms has elevated the significance of drug delivery systems that simulate the symptomatic need of disease. Such considerations have refocused attention of pharmaceutical scientists to idealized drug delivery where the necessary quantity of active agent is delivered at the appropriate time and place of action in the body [64].

In the CDDS, the drug is released and maintained in the body at the needed concentration by using only two parts in the delivery agent. Loading dose should be delivered out at the start and maintenance dose at the end. A fast pharmacological effect is achieved by a high initial loading dose and a constant slow release of the drug ensures the reaction duration is maintained. The rate at which the drug is given in maintenance should be the same as the rate at which it is excreted from the body [65] [66].

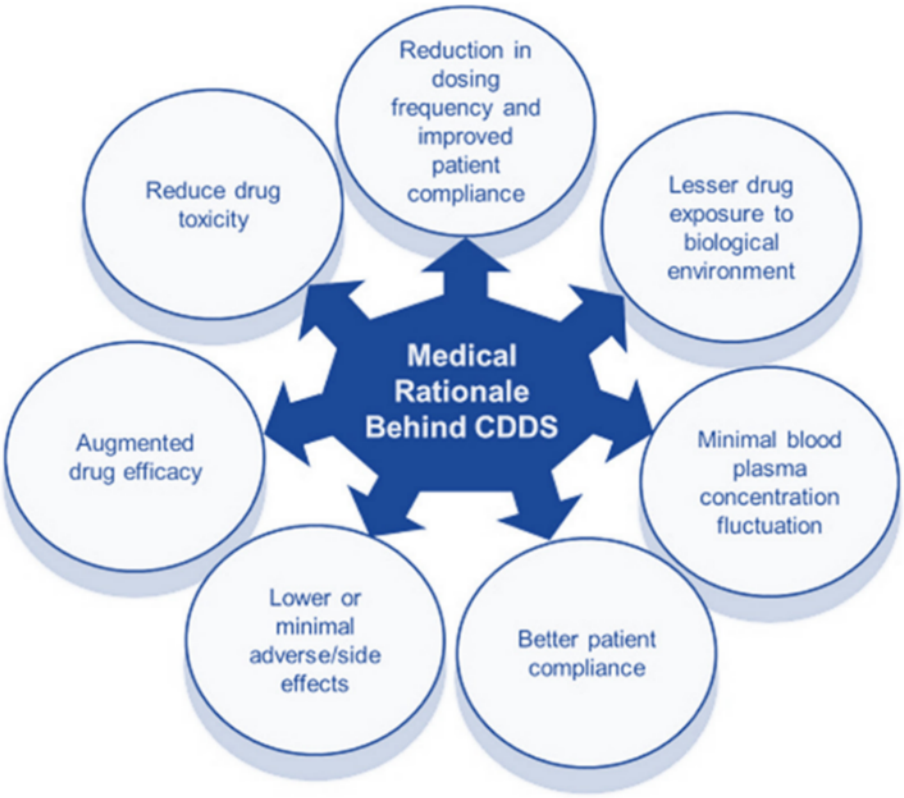

FIGURE 2.5: Advantages of developing CDDS [11].

2.8 Polymers

Natural polymers or the biopolymers are often obtained from both plants and animals [67]. These polymers are important for forming tissues in the body and signaling the human endocrine system, among their various roles. As a result, natural materials are a great option for making hydrogels due to their known biological properties, but their difficult synthesis, mechanical properties, and instability are considered their greatest challenges [68].

The controlled drug release from natural polymers enhances treatment effectiveness and reduces negative side effects. Natural polymers can be engineered to react to pH, temperature or enzymes in the body, allowing drugs to only be released in the intended region [69].

As a result, the amount of drug given can be minimized, lessening side effects and providing better safety for patients than standard synthetic drugs [11]. Table 2.1 summarizes the use of natural and synthetic polymers in drug delivery.

Synthetic polymers poly (N-isopropylacrylamide) (PNIPAM), polyethylene glycol (PEG), and poly(acrylic acid) (PAA), are used to formulate nanogels with stimuli-responsive features which are sensitive to temperature, pH, or redox state. These polymers increase the ability of nanogels to target drugs to specific diseases, like a tumor or an inflamed area, where the environmental conditions trigger the release of drugs.

Polysaccharides chains have abundant hydroxyl functions and/or other functional groups (amino, carboxylic, and so on), giving a wide range of possibilities to synthesize polymer-based hydrogels by chemical or physical cross-linking. Synthetic polymers have the advantage in certain aspects like tunable properties, unlimited shapes, and known structures to natural polymers.

Synthetic biomaterials may enhance the prevention or reversal of impaired or defected tissue structure and tissue function. They are easily synthesized compared

to naturally occurring polymers because of polymerization, interlinkage, and functionality (block structures, combination, copolymerization) of molecular weight, molecular structure, physical and chemical properties [70, 71].

The disadvantage with the use of synthetic biomaterials is that they cannot be adsorbed by cells and must be chemically treated to allow greater attachment of cells. Numerous commercial synthetic polymers have similar physiochemical and mechanical properties with those of biological tissues [72].

TABLE 2.1: Comparison of Natural and Synthetic Polymers

Natural Polymers	**Synthetic Polymers**
Advantages	
• Less toxic • Biocompatibility • Biodegradable • Easily available • Inherently bioactive	• Easily reproducible • Customizable composition • Higher mechanical strength • Better structural stability • More economical
Disadvantages	
• High degree of variability in natural materials derived from animal sources • Structurally more complex • Extraction process very complicated and high cost • Poor mechanical properties • Insufficient mechanical strength	• Toxic • Non-degradable • Synthetic process is very complicated • Lacks bioactivity
Examples	
Cellulose, starch, chitosan, carrageenan, alginates, xanthan gum, gellan gum, pectins	poly(lactic acid) (PLA), poly(acrylic acid), poly(anhydrides), poly(amides), poly(ortho esters), poly(ethylene glycol), poly(vinyl alcohol) (PVA), poly(ethylene oxide) (PEO)

2.9 Xanthan Gum

Xanthan gum (XG) is a natural, anionic extracellular polysaccharide with wide pharmaceutical applications. XG polymeric networks have been used as drug carriers for the administration of numerous drugs. Its hydrophilic matrix prolongs residence time in gastrointestinal tract, providing controlled drug release [12].

XG consists of D-glucose linked in β-(1→4) order, with a side chain of β-D-mannose attached to the D-glucuronic acid-beta glucuronic acid-D-mannose linked to C-3 on these glucose units, as represented in Figure 2.6 [73].

XG is more thermally resistant to hydrolysis or degradation than other water-soluble polysaccharides, a property attributed to the complex, uniform XG structure, which does not allow the molecules to depolymerize. XG polymer is soluble in water, which can be used as a dispersion stabilizer, wetting agent, viscosity increasing agent, gelling agent etc. It has a number of applications in food, pharmaceutical and biomedical industries [74].

Xanthan gum is more comfortable and safe to work in the pharmaceutical area due to its pulsated drug release at the specific pH and temperature at the targeting point. As peculiar polymeric features, the polysaccharides belong to the physiologically hetero-polysaccharides, and demonstrate the remarkable biological properties, in particular, nontoxic, bioadhesive [75].

Antioxidant, biocompatibility, hemostatic, antimicrobial, mucoadhesion, cytocompatibility, these polysaccharides have been applied in many fields such as solid oral dosage form, ophthalmic, buccal, topical, nasal, and advanced drug delivery [76].

It is a better alternative to synthetic polymers because it is biocompatible, readily available and non-toxic. It demonstrates great stability in low pH, which can prevent the degradation of the drug in the stomach and liberate the drug in an alkaline environment. XG has a natural mucoadhesive characteristic, this improves the retention time of the drug and improves its therapeutic activity [13].

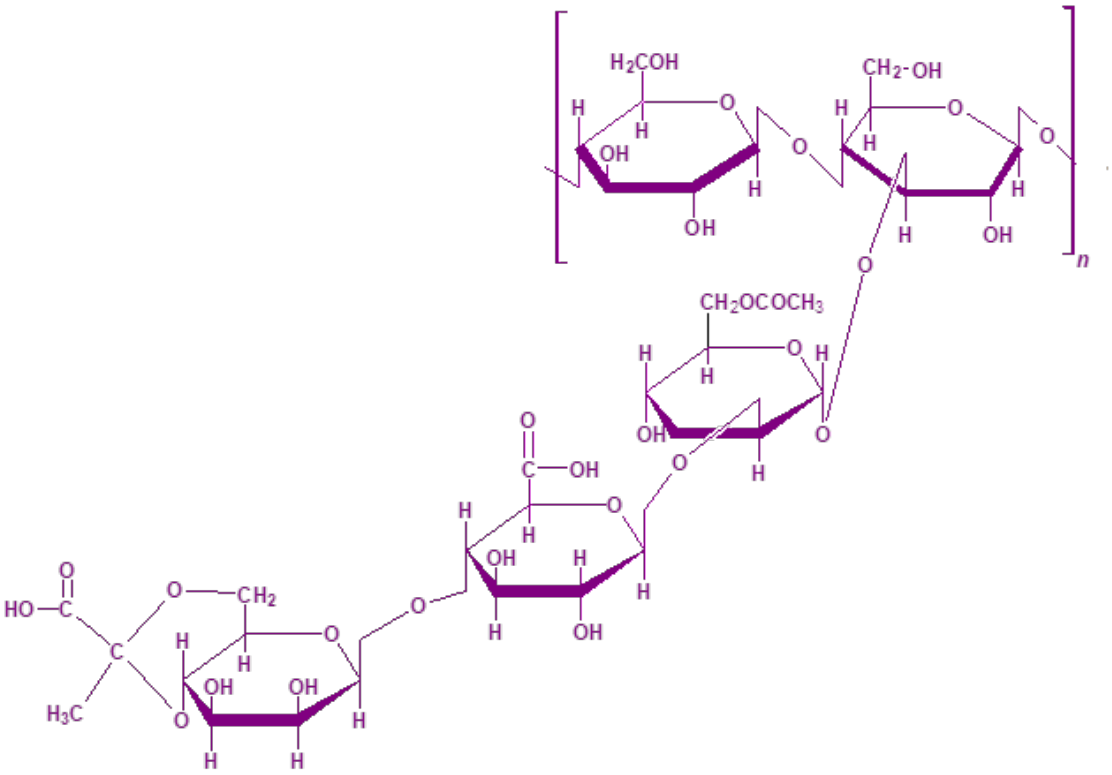

FIGURE 2.6: Structure of XG.

As a result, this polymer has been thoroughly investigated for a wide range of pharmaceutical and biological applications in recent years.

In this regard, a range of formulations based on XG showed encouraging outcomes for several applications, such as hydrogels for the administration of different medications [12], transdermal patches [77], vaginal delivery [78], anticancer drugs [16], controlled-release tablets [17], and periodontal diseases [79]. Figure 2.7 represents the benefits of using XG in drug delivery systems.

Hydrogels made from XG have been found useful in drug delivery, by helping control the release of different types of drugs. Due to its hydrophilicity, it enhances swell-ability of the hydrogels. When XG is linked to polymeric chains, it produces strong elastic gel that gives tight control over the release of the drug and has zero order kinetics, making them ideal for controlled drug delivery of various medications [80].

FIGURE 2.7: Advantages of XG in drug delivery systems.

When drugs are given in a conventional form, they often have low bioavailability because they are quickly excreted from the upper part of the GIT. Improved bioavailability for these drugs can be achieved using drug delivery systems that decrease the time they take to pass through the stomach.

XG by itself or together with other polymers has commonly been used in the manufacturing of gastroretentive formulations. Instead of allowing gas to float, the gel traps it inside the stomach which helps food stay in the stomach longer [13].

The ability of XG to attach to mucus means it can be applied to gastro-retentive and other drug delivery systems such as formulations for the nose, mouth, eyes and skin. XG has also been used to produce gastroretentive matrix tablets that expand in the stomach using a range of in situ gelling polymers [81].

A study was conducted to inspect the impact of XG on gelatin-CMC blend. When XG and gelatin-CMC blends are combined, the resulting films display improved UV protection, transparency, improved mechanical strength and resistance to punctures. The formulation containing 5% xanthan gum showed the best properties, indicating XG improves the performance and compatibility of CMC-based systems in pharmaceutical or packaging applications [82].

2.10 Carboxymethyl Cellulose

Carboxymethyl cellulose (CMC) is a cellulose derivative polymer. It plays a major role in the biomedical field. It is both biocompatible and water-soluble. For this reason, it is applied across a variety of industries. When CMC is crosslinked, the resulting hydrogels are biodegradable, have strong water-retention qualities and are safe [83].

CMC is highly promising to be applied in drug delivery system development owing to its physicochemical attributes, biocompatibility, biodegradability, and low immunogenicity. CMC can absorb large amounts of water and swell to form polymeric networks with desired properties when cross-linked with an appropriate polymer or monomer [84].

Studies have shown when different polymers and crosslinking agents were added to CMC, the resulting composite hydrogels provided target, controlled and efficient drug delivery. Due to their strong pH sensitivity, the hydrogels can be used effectively for purposely targeted delivery of drugs [85]. The chemical structure of CMC is illustrated in Figure 2.8.

Yu Han *et al.*, prepared a double-layer hydrogel systems using alginate and CMC, resulting in a sustained released drug delivery system and prevented drug from leaking as single-layer systems did. This approach gave promising results for drugs that are hydrophobic or form macromolecules [86]. Ashames. A, *et al* created hydrogels incorporating AMPS with CMC/PVP, to provide release of the drug in alkaline conditions at pH 6.8. When subjected to various physiological

environments, the hydrogel exhibited superior stability and is more swollen at pH 6.8 compared to acidic environment i.e., pH 1.2. The hydrogels showed better performance at 6.8 pH than at 1.2 pH and steadily released medication for about 24 hours, providing a sustained release system [87].

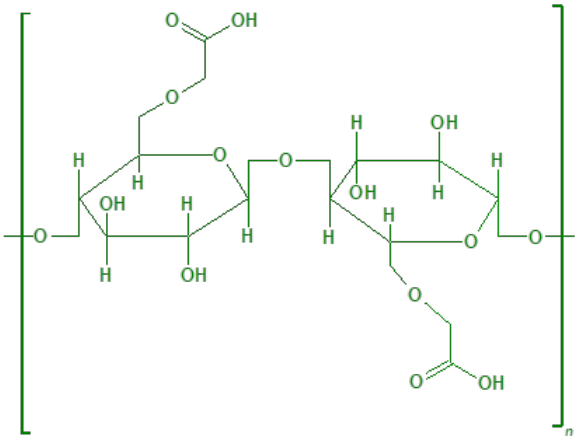

FIGURE 2.8: Structure of CMC.

Hydrogels made from carboxymethyl cellulose (CMC) load drugs efficiently and swell well, but their mechanical strength is notably low. It has been demonstrated that combining CMC with other polymers, such as carboxymethyl β-cyclodextrin (cmβCD) can provide improved mechanical strength with efficient loading and providing controlled release of the drug. Such combinations are suitable for safe and effective use in CDDS applications [88]. The results demonstrate that combining CMC with other polymers helps improve the effectiveness of sustained release drug delivery systems.

2.11 Acrylic Acid

Acrylic acid (AA) is a type of pH-sensitive, synthetic polymer commonly used for targeted drug delivery in the gastrointestinal tract. This polymer is considered a key superabsorbent and is often called a pH-responsive polyelectrolyte. Changing the polymer components can modify the initial pH-dependent release capability. Consequently, there have been many studies on pH-responsive polymeric networks [8]. Polymers made from acrylic acid are also known to respond to both thermal,

electrical and pH changes [9]. Due to its polyanionic nature, poly (acrylic acid) is broadly utilized to create macromolecules that respond to changes in pH and are used mainly for targeted drug delivery [10]. With a pKa ranging between 4.5 and 5.0, poly (acrylic acid) strongly swells in water at physiological pH because of its carboxylic acid groups becoming ionic [11]. The structure of AA is illustrated in Figure 2.9.

Bukhari SMH, *et al.* prepared a pH sensitive system using AA as monomer and gelatin. They found that when the amount of AA in the system increased, the pH sensitive hydrogels showed higher swelling due to the electrostatic repulsion caused by COO- ions of AA [89]. Pervaiz, Fahad, *et al.* conducted a study with the objective of development and characterization of polyethylene glycol (PEG) and XG and AA based interpenetrating network (IPN) in the controlled release of venlafaxine. They have observed that, higher AA content exhibits high swelling because of (–COO-) repulsion in the dissolution medium that further leads to higher drug release profile [90].

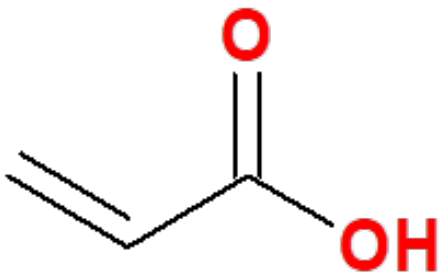

FIGURE 2.9: Structure of AA.

2.12 Comparative Analysis of TGR-Based Pharmaceutical Formulations

Table 2.2 describes several formulation approaches that researchers have investigated to improve the therapeutic action of TGR, a BCS Class IV drug with major solubility and dissolution problems. This review discusses the conventional and novel approaches to drug delivery, including solid dispersions, lipid formulations,

nanosuspensions, and polymer carriers. Every entry describes the type of formulation, important materials such as polymers or surfactants, objectives, and the central outcomes. As the comparison covers the important details, it becomes easier to find previously successful methods, while also finding unaddressed issues.

TABLE 2.2: Overview of Ticagrelor-Based Drug Delivery Systems in Literature.

Authors	**Year**	**Polymer (s)**	**Formulation Type**	**Objective**	**Key Findings / Outcome**	**Ref.**
Usman Saleem, *et al.*	2024	PVA, AMPS	Nanogel	Enhance solubility & dissolution of TGR	99.91% drug release; improved solubility	[91]
Anam Aziz, *et al.*	2024	PEG	Self-nanoemulsion	Improve solubility & permeability	Solubility & permeability improved vs pure drug	[92]
Patel, *et al.*	2024	HPMC	Matrix Tablets	Develop sustained release tablets	Extended release profile achieved	[93]
U. Shastri, *et al.*	2024	PEG-600	Liquisolid Tablets	Enhance solubility & release	82–96% release, <10 min disintegration	[94]
Alsafar, Z.F., *et al.*	2023	PEG	Nano-Micelles	Improve solubility & permeability	High stability in GIT; effective ex vivo diffusion	[95]
Ahmed A.A. Alsaad	2022	HPβCD	CD Complex	Enhance solubility & dissolution	10× increase in solubility	[96]
Shahid, *et al.*	2022	Chitosan	Nanoparticles	Mucoadhesive controlled release for bioavailability	Improved solubility, stability, bioavailability	[97]
Khalid & Abd Alhammid	2022	PEG	Nanoemulsion	Enhance solubility & bioavailability	Improved aqueous solubility & bioavailability	[98]
Shahid, *et al.*	2022	Thiolated chitosan	Nanoparticles	Improve mucoadhesion & bioavailability	Sustained release & enhanced bioavailability	[99]
Vadapalli & Reddy	2022	PEG + co-surfactants	SMDDS	Enhance solubility	Improved solubility & dissolution	[100]

Table 2.2 continued from previous page

Authors	Year	Polymer (s)	Formulation Type	Objective	Key Findings / Outcome	Ref.
Hosseini-Ashtiani & Tadjarodi	2021	Chitosan	Nanoparticles	Controlled release oral formulation	Sustained release achieved	[101]
Linkun Hao, *et al.*	2021	PLGA	Injectable microspheres	Develop sustained-release system	Good in vitro release profile	[102]
Shahid, *et al.*	2021	Chitosan, Acrylic acid	pH-Responsive NPs	Enhance oral bioavailability	Controlled pH response & improved bioavailability	[103]
Zaman, *et al.*	2021	Thiolated hemicellulose	-	Study mucoadhesion & dissolution	Good mucoadhesion & release	[104]
Yadav, *et al.*	2021	PEG	Solid dispersion	Improve absorption & permeability	High release, permeability & bioavailability	[105]
Na, *et al.*	2020	PVA, PEG	Nanosuspension	Enhance dissolution & bioavailability	2.8-fold increased GI absorption vs commercial product	[106]
Zaman, *et al.*	2020	Thiolated β-CD	Tablets	Study β-CD as excipient	96.62% release in 1 hour; biocompatible	[107]
Mohammed & Ghareeb	2018	PVP, Poloxamer 188, HPMC	Nanoparticles	Improve solubility & dissolution	HPMC gave smallest size; improved dissolution	[108]

Note: PVA: Polyvinyl Alcohol; AMPS: 2 - Acrylamido - 2 - methylpropane Sulfonic Acid; PEG: Polyethylene Glycol, HPβCD: Hydroxypropyl Beta - Cyclodextrin; HPMC: Hydroxypropyl Methylcellulose; PVP: Polyvinylpyrrolidone; PLGA: Poly(lactic - co - glycolic acid); β-CD: Beta - Cyclodextrin, PEG-600: Polyethylene Glycol (MW 600).

Chapter 3

Material and Methods

3.1 Materials

TGR (TGR) was generously provided as a gift sample by Horizon Pharmaceuticals (Pvt.) Ltd., Islamabad, Pakistan. Carboxymethylcellulose sodium (CMC, high viscosity, USP grade) and xanthan gum (XG, pharmaceutical grade) were procured from Sigma-Aldrich (St. Louis, MO, USA). N, N′-Methylenebisacrylamide (MBA, ≥99% purity) and acrylic acid were obtained from Merck KGaA (Darmstadt, Germany). Ammonium persulfate (APS, ≥98% purity, molecular biology grade) was purchased from Thermo Fisher Scientific (Waltham, MA, USA). Sodium hydroxide (NaOH, ≥97%, analytical grade), potassium dihydrogen phosphate (KH_2PO_4, ≥99%, ACS reagent grade), and absolute ethanol (HPLC grade) were sourced from Sigma-Aldrich (Germany). All chemicals were used as received without further purification. Freshly distilled water was prepared using a Milli-Q water purification system (Millipore, Bedford, MA, USA) at the Faculty of Pharmacy, Capital University of Science and Technology (CUST), Islamabad, Pakistan.

3.2 Method

The hydrogels were synthesized using the free radical polymerization method. A schematic representation of the hydrogel synthesis process is provided in Figure 3.1.

This procedure involved systematically varying the ratios of polymer, monomer, and cross-linker, as detailed in Table 3.1, to evaluate the effect of concentration variations on the final hydrogel properties. Separate aqueous solutions of carboxymethyl cellulose (CMC), xanthan gum (XG), acrylic acid (AA), N,N-methylenebisacrylamide (MBA), and ammonium persulfate (APS) were prepared using distilled water. The typical concentrations of CMC, XG, AA, and MBA employed are summarized in Table 3.1. The CMC solution was gradually incorporated into the XG solution under continuous stirring at 500 rpm and 25 ± 1^{o}C for 15 minutes to obtain a homogeneous polymer matrix. Separately, the AA and APS solutions were stirred at 600 rpm and 25 ± 1^{o}C to ensure complete dissolution.

The APS initiator solution (0.1 M) was subsequently added to the AA monomer solution and stirred for 7 ± 2 minutes to facilitate free radical generation. After cooling the CMC/XG polymer blend to 25 ± 1^{o}C, the activated AA/APS mixture was transferred into the polymer solution and homogenized at 600 rpm for 20 minutes to achieve a clear, uniform mixture. The MBA cross-linker solution, prepared in a 2:1 (v/v) mixture of distilled water and ethanol, was then added dropwise at a controlled rate of 0.5 mL/min under a nitrogen atmosphere to minimize oxygen inhibition of the radical polymerization process. This step was conducted at 50 ± 1^{o}C with continuous stirring at 400 rpm. The final mixture was transferred to a water bath maintained at 70 ± 1^{o}C and allowed to undergo gelation for 4.5 ± 0.5 hours, completing the formation of the cross-linked hydrogel network.

The synthesized hydrogels were cut into uniform cylindrical. Residual unreacted materials were removed by sequential washing with a 1:1 (v/v) mixture of distilled water and ethanol for three cycles of 24 hours each. The purified hydrogels were subsequently lyophilized using a lyophilizer at –80^{o}C under a vacuum of 0.01 mbar

for 48 hours to obtain dry, stable formulations suitable for further characterization [91, 109].

TABLE 3.1: Experimental Design and Composition of Formulations

Formulation	Polymers		Monomer	Cross-linker	Initiator
	CMC	XG	AA	MBA	APS
F1	1	2	4	0.3	0.5
F2	2	2	4	0.3	0.5
F3	3	2	4	0.3	0.5
F4	1	4	4	0.3	0.5
F5	1	6	4	0.3	0.5
F6	1	2	8	0.3	0.5
F7	1	2	12	0.3	0.5
F8	1	2	4	0.5	0.5
F9	1	2	4	0.7	0.5

3.3 Drug Loading

A 0.3% (w/v) solution of TGR was prepared in phosphate-buffered saline (PBS, pH 7.4). Precisely weighed hydrogel discs were immersed in the drug loading solution of 100mL and incubated at 37^{o}C ($\pm$0.5^{o}C) under static conditions for 48 h. Following incubation, hydrogels were removed, rinsed with fresh PBS (3 $\times$ 5 mL), and dried to constant weight at 25^{o}C under vacuum. Drug loading efficiency (%) was determined via UV-Vis analysis. Loaded hydrogels underwent subsequent physicochemical characterization [110].

3.4 Characterization

3.4.1 Drug Entrapment Efficiency

The hydrogel disc was weighed and placed into a solution prepared by mixing methanol and distilled water in a 1:1 ratio. Then it was stirred at 13000 rpm for 60 min on a magnetic stirrer, at a temperature range of 25^{o}C $\pm$ 1. This was

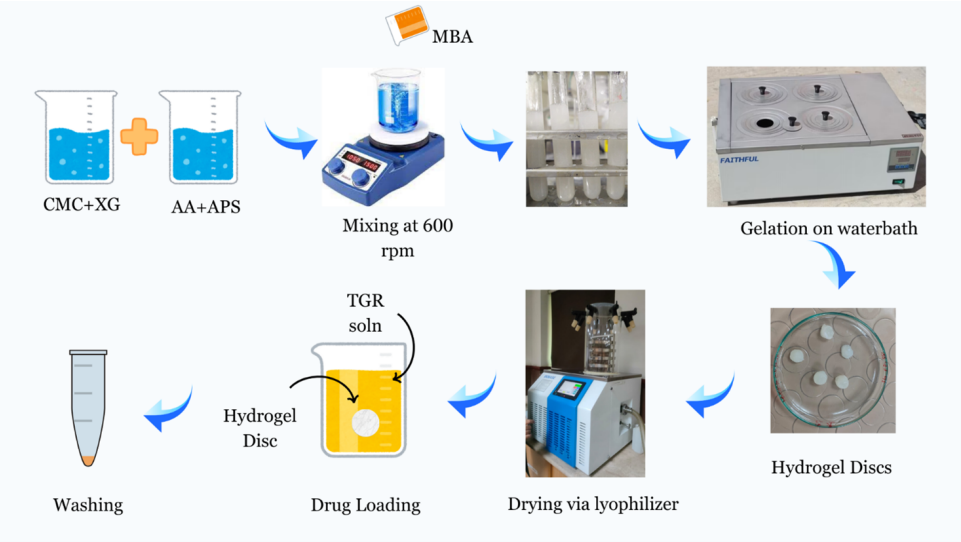

FIGURE 3.1: Schematic Representation of Hydrogel Formulation Process.

followed by a collection of the supernatants, and filtration of the supernatants was carried out using a membrane filter of size 0.45 μm and further analyzed by spectrophotometry at 255 nm (λmax). According to the calibration curve, the drug concentration was quantified [111, 112]. The % DEE was calculated using equation 1:

$$EE\% = \frac{Total\ drug - Free\ drug}{Total\ drug} \times 100 \tag{3.1}$$

3.4.2 *In-Vitro* Swelling Studies

A swelling study of the formulated hydrogels was performed in simulated gastric fluid (SGF) at pH 1.2 and simulated intestinal fluid (SIF) at pH 6.8. The impact of the medium on the swelling behavior of hydrogels was determined by recording dynamic changes of swelling at predetermined time intervals. Weighed discs of hydrogels were immersed in 100 mL of 0.5M buffer solution adjusted at pH 1.2 and 6.8. The swollen discs, after a predetermined time, were removed from the buffer solution, and the Whatman's filter paper was used to properly clean surface media. The swollen discs' weight was recorded using a weighing balance. Afterwards, the discs were re-soaked into their respective beakers. This procedure was repeated until the weight was at equilibrium. The swelling study was observed for 32 h

[113]. The swelling index was calculated using equation 2:

$$Swelling\ Index = \frac{w_2 - w_1}{w_1} \tag{3.2}$$

Where W1 is the dried hydrogel weight and W2 is the weight of hydrogel at the swollen state.

3.4.3 *In-Vitro* Drug Release Study and Drug Release Kinetics

Dissolution profiles of TGR-loaded hydrogel formulations were carried out in solutions of SGF pH 1.2 and SIF pH 6.8. The USP Dissolution Apparatus II (paddle) was used for the drug release studies, at 37 ± 0.5^{o}C and 50 rpm stirring. Drug-loaded hydrogels in precisely weighed quantities were placed in 900 mL of pH 1.2 and pH 6.8 solutions, respectively. Samples were withdrawn from each basket at predetermined intervals and replaced with an equal volume (5 mL) of completely new dissolution medium. All the samples were filtered through a membrane filter with a 0.45 μm diameter, and the drug release was analyzed using spectrophotometric measurement at 255 nm λmax after appropriate dilution [114].

The drug release kinetics of TGR-loaded hydrogels was explored with the help of mathematical models using % drug release versus time data. Different kinetic models, including first-order, Higuchi, zero-order, Weibull, and Korsmeyer-Peppas models, were employed for the study of the drug release behavior of the formed hydrogels [115].

3.4.4 Fourier Transform Infrared Spectroscopy

The Fourier transform infrared (FTIR) spectra of XG, CMC, AA, pure drug (TGR), and drug-loaded hydrogels were recorded using a Nicolet iS50 FTIR spectrometer (Thermo Fisher Scientific, Waltham, MA, USA) equipped with an attenuated total reflectance (ATR) accessory. Powdered samples were directly placed on

the ATR crystal. Spectra were acquired over the wavenumber range of 4000–500 cm^{-1} with a resolution of 4 cm^{-1}, averaging 32 scans per sample [116].

3.4.5 Thermal Stability Analysis

The thermal properties of the prepared hydrogels and individual components were assessed using differential scanning calorimetry (DSC) and thermogravimetric analysis (TGA). DSC analysis was conducted using a Q2000 differential scanning calorimeter (TA Instruments, New Castle, DE, USA). Approximately 5.0 ± 0.5 mg of each sample (n = 3) was accurately weighed and hermetically sealed in standard aluminum pans. Thermal scans were performed over a temperature range of 30^{o}C to 281^{o}C at a heating rate of 10^{o}C/min under a nitrogen atmosphere with a flow rate of 25 mL/min. TGA was carried out using a TGA 5500 thermogravimetric analyzer (TA Instruments, New Castle, DE, USA). Approximately 9.0 ± 0.5 mg of powdered hydrogel was placed in a platinum crucible. The samples were heated from 30^{o}C to 600^{o}C at a rate of 10^{o}C/min under a constant nitrogen purge of 35 mL/min. Thermograms were recorded to assess thermal stability and degradation behavior [117].

3.4.6 Powder X-ray Diffraction Analysis

The crystalline structure of individual components and hydrogel formulations was evaluated using an X-ray diffractometer (D8 Advance, Bruker, Billerica, MA, USA) with Cu Kα radiation (λ = 1.5406 Å). Samples were packed into zero-background silicon sample holders. Diffraction patterns were collected over a 2θ range of 3^o to 70^o using a step size of 0.02^o and a counting time of 1 second per step [118].

3.4.7 Scanning Electron Microscope

The surface morphology of vacuum-dried hydrogel formulations was examined using a scanning electron microscope (JSM-IT800, JEOL Ltd., Tokyo, Japan).

The samples were mounted on aluminum stubs with carbon adhesive tape and sputter-coated with a 15 nm layer of gold-palladium using a Q150T ES sputter coater (Quorum Technologies, Laughton, UK) to enhance conductivity. The images were captured at an accelerating voltage of 5 kV to observe surface topology and microstructural features. Images were then captured under different levels of magnification [119].

3.4.8 Acute Oral Toxicity Studies

To evaluate the biocompatibility of the synthesized hydrogels, an acute oral toxicity study was performed in accordance with OECD Guideline 423 and with strict adherence to the ARRIVE 2.0 guidelines. The experimental protocol received prior approval from the Ethics Review Committee of Capital University of Science and Technology (CUST), Pakistan (Ref# REC/FoP/F2024/09).

Ten healthy adult albino mice (Balb/c strain), weighing 25–35 g, were procured from the CUST animal facility. Animals were acclimatized for seven days under standard laboratory conditions (12-hour light/dark cycle, 25 $\pm$ 2^{o}C temperature, 65 $\pm$ 5% relative humidity) with free access to a standardized diet and water.

Following acclimatization, animals were randomly divided into two groups (n = 5 per group). Group A (Control) received 0.9% normal saline at a dose of 1 mL/100 g body weight via oral gavage. Group B (Test Group) received the TGR-loaded hydrogel at 2g/kg body weight dose, administered via oral gavage to fasted animals. Both control and test formulations were freshly prepared in sterile 0.9% saline prior to administration.

Post-administration, animals were observed continuously for the first four hours and subsequently monitored daily for 14 days. Clinical observations included assessment of mortality, changes in skin, fur, eyes, mucous membranes, respiration, salivation, diarrhea, tremors, convulsions, posture, gait, coma, grooming behavior, and other neurological or behavioral abnormalities, using a standardized scoring system. Body weight and food/water intake were recorded daily.

On day 14, all animals were euthanized under anesthesia. Blood samples were collected via cardiac puncture for hematological analysis (RBC, WBC, hemoglobin, hematocrit, platelet count, differential leukocyte count) and serum biochemical evaluation (ALT, AST, ALP, blood urea nitrogen, creatinine, total protein, albumin, glucose) using validated diagnostic kits. Major organs, including the heart, liver, kidneys, spleen, stomach, and lungs were visually examined for gross abnormalities, and preserved in 10% neutral buffered formalin for histopathological evaluation.

Fixed tissues were processed using standard paraffin-embedding techniques, sectioned at 5 μm thickness, and stained with hematoxylin and eosin (H&E) [120]. Histopathological evaluation was performed by a pathologist blinded to the treatment groups, with lesions graded semi-quantitatively as follows: 0 (absent), 1 (minimal), 2 (mild), 3 (moderate), and 4 (severe).

3.5 Statistical Analysis

All data were presented as mean values with standard deviation. Statistical analysis was performed using SPSS ® software. A one-way analysis of variance (ANOVA) was applied for comparisons involving more than two groups followed by an appropriate post-hoc test, while Student's t-test was used for direct comparisons between two groups. A significance level of $P < 0.05$ was used to determine statistical significance.

Chapter 4

Results and Discussion

4.1 Entrapment Efficiency

The entrapment efficiency (EE) of the synthesized hydrogel formulations (F1-F9) showed a clear compositional dependence on the levels of carboxymethyl cellulose (CMC), xanthan gum (XG), acrylic acid (AA), and the crosslinking reagent N,N-methylene bisacrylamide (MBA), which is expressed in Table 4.1 and Figure 4.1. One-way ANOVA of statistical analysis between formulations indicated that there were significant differences between the formulations percent encapsulated drug ($p = 0.0069$), demonstrating that polymer architecture and crosslinking density played a crucial role in drug encapsulation. Formulation F1, which had 1% CMC and 2% XG, had a moderate % EE of 73.10 ± 0.93%, which acted as a baseline. The% EE exhibited a slight elevation to 76.60 ± 0.80 percent only when the concentration of CMC was raised to 2% in F2, which indicated that CMC at moderate concentrations provide minor structural contributions. An additional increase in CMC up to 3% in F3 showed a considerable decline in %EE value to a relatively low 70.20 ± 0.62, due to the high viscosity given by the high CMC content, which would hinder uniform diffusion and distribution of the drug in the hydrogel matrix [121]. Conversely, formulations F4 and F5, with XG concentration elevated to 4 and 6 percent, respectively, whereas CMC, AA, and MBA were kept at a constant level, demonstrated a significant difference in %EE, 84.70 ± 0.76

and 90.40 ± 0.52, respectively. The maximal %EE achieved in F5 was perhaps as a result of the best addition of XG, which increased porosity, hydration, and swelling potential; hence the high drug entrapment seen in Figure 4.1 clearly [122]. Similarly, %EE was significantly affected by the concentration of AA, as observed in formulations F6 and F7 upon the increase of AA to 8% and 12%, resulting in values of %EE at 80.50 ± 0.73 and 87.30 ± 0.50, respectively. Higher AA concentrations improved entrapment, which was attributed to an increase in ionic crosslinking, swelling-mediated porosity, and the consequent ability to retain the drug well and provide effective entrapment. The %EE of F7, however, showed less %EE than F5 despite its AA being elevated, indicating that the role of XG in network formation and drug entrapment was greater than that of AA alone. An inverse relationship between MBA concentration and %EE was also highly evident in formulations F8 and F9, where higher percentage amounts of crosslinker (0.5% and 0.7%, respectively) decreased the %EE to 65.60 ± 0.68 and 62.80 ± 0.61, respectively. This was probably due to the excess crosslinking that formed a high-density rigid polymer network with limited free volume and swelling capacity that limited the amount of drug to be entrapped [121].

These results were comparable to the earlier reported results, as higher levels of over-crosslinked hydrogel matrices showed lower porosity and a low loading capacity of drugs. The general outcome showed that the formulations with the maximum swelling and porosity, like F5 and F7, had the best %EE, whereas formulas showing high viscosity levels (F3) or over-crosslinked networks (F8 and F9) displayed reduced entrapment efficiency. All these findings underlined the significance of optimizing the polymer and crosslinker ratio to have a desirable balance between mechanical stability, swelling characteristics, and drug retention, thus to develop optimal hydrogel-based drug delivery systems with a maximized entrapment capacity and functionality [123].

Table 4.1: Entrapment Efficiency (% EE) of Hydrogel Formulations.

Formulation	**% EE**
F1	73.1 ± 0.93
F2	76.6 ± 0.80
F3	70.2 ± 0.621

Table 4.1 continued from previous page

Formulation	% EE
F4	84.7 ± 0.76
F5	90.4 ± 0.52
F6	80.5 ± 0.73
F7	87.3 ± 0.50
F8	65.6 ± 0.68
F9	62.8 ± 0.61

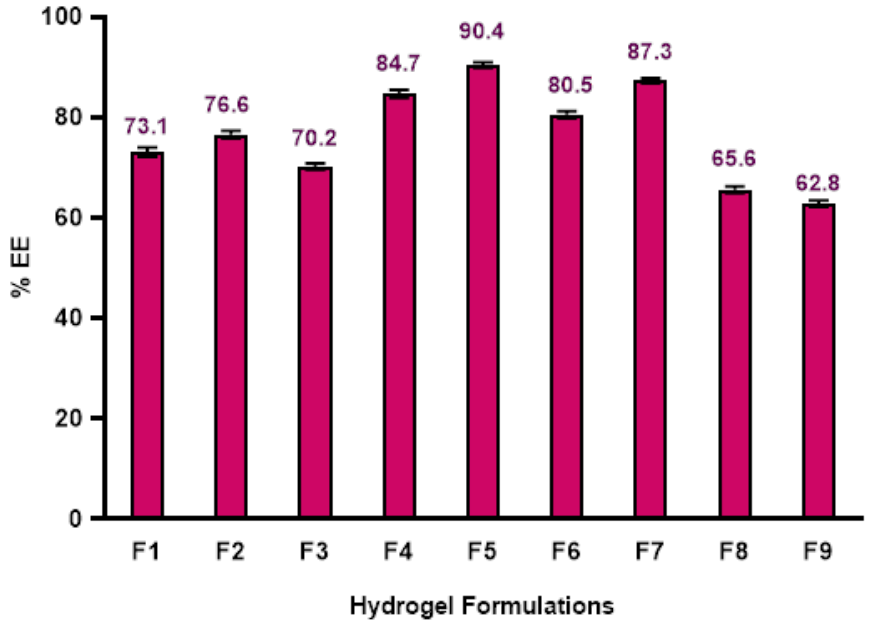

FIGURE 4.1: % Drug Entrapment Efficiency of Hydrogel Formulations (F1-F9).

4.2 *In-Vitro* Drug Release and Drug Release Kinetics

In vitro drug release profiles of the prepared hydrogel formulations (F1-F 9) were evaluated systematically under simulated gastric fluid (SGF, pH 1.2) and simulated intestinal fluid (SIF, pH 6.8) to determine the pH-sensitive characteristic of these formulations. The difference observed between the release of the different formulations of the drug and under varied pH conditions was significant ($p < 0.05$), which confirmed the pH-sensitive behavior of the hydrogels prepared. Drug

release at the acidic pH (1.2) varied between 20.56% ± 0.42 (F9) and 48.75% ± 0.51 (F5), and at pH 6.8 there was a significant increase in drug release, varying between 50.27% ± 0.63 (F9) and 86.83% ± 0.45 (F5), as shown in Figure 4.2. These data are given as mean SD values because the experiments were done in triplicate (n = 3) to make it statistically valid.

The highest drug release was observed with F5 (86.83% ± 0.45), then F7 (84.79% ± 0.49), and F4 (80.21% ± 0.57) than any other formulation at the physiologic condition of pH 6.8. Conversely, formulation F9 showed the lowest releasing effect at both pH levels because it contained a higher concentration of crosslinker MBA (0.7% w/w) which increased the density of the tightened crosslinked hydrogel structure and therefore limited drug diffusion [124].

Comparative analysis of formulations showed significant increments in drug release when xanthan gum (XG) content was increased from 2 g (F1) to 6 g (F5) at both pH levels, and this can be explained by increased swelling capacity with increasing polymer content [125].

Likewise, a difference in concentration of acrylic acid (AA) had a linear effect on drug release. F7 with higher AA concentration offered better drug release as expected because of increased ionization as well as swelling in the presence of alkaline conditions [126].

On the other hand, formulations F8 and F9, which held higher concentrations of MBA (0.5% w/w, and 0.7% w/w, respectively), indicated limited drug release, especially at pH 6.8, as illustrated by the inverse correlation between crosslink density and the rate of drug release [124].

Interestingly, even with a higher amount of CMC, F3 had lower drug release (28.18% ± 0.46 at pH 1.2 and 60.17% ± 0.52 at pH 6.8), perhaps because of the lesser amount of XG and the corresponding effect on the swelling dynamics, which reflects the strong impact of polymer balance on drug release behavior. The drug release trends shown in Figure 4.2 show well the pH-responsive release behavior of hydrogels, where lower release is observed in the gastric conditions and the increased drug release occurs at the intestinal pH conditions. This would be due

to the deprotonation of carboxylic acid groups at an increased pH, which causes electrostatic repulsion of the network and subsequent drug diffusion [127].

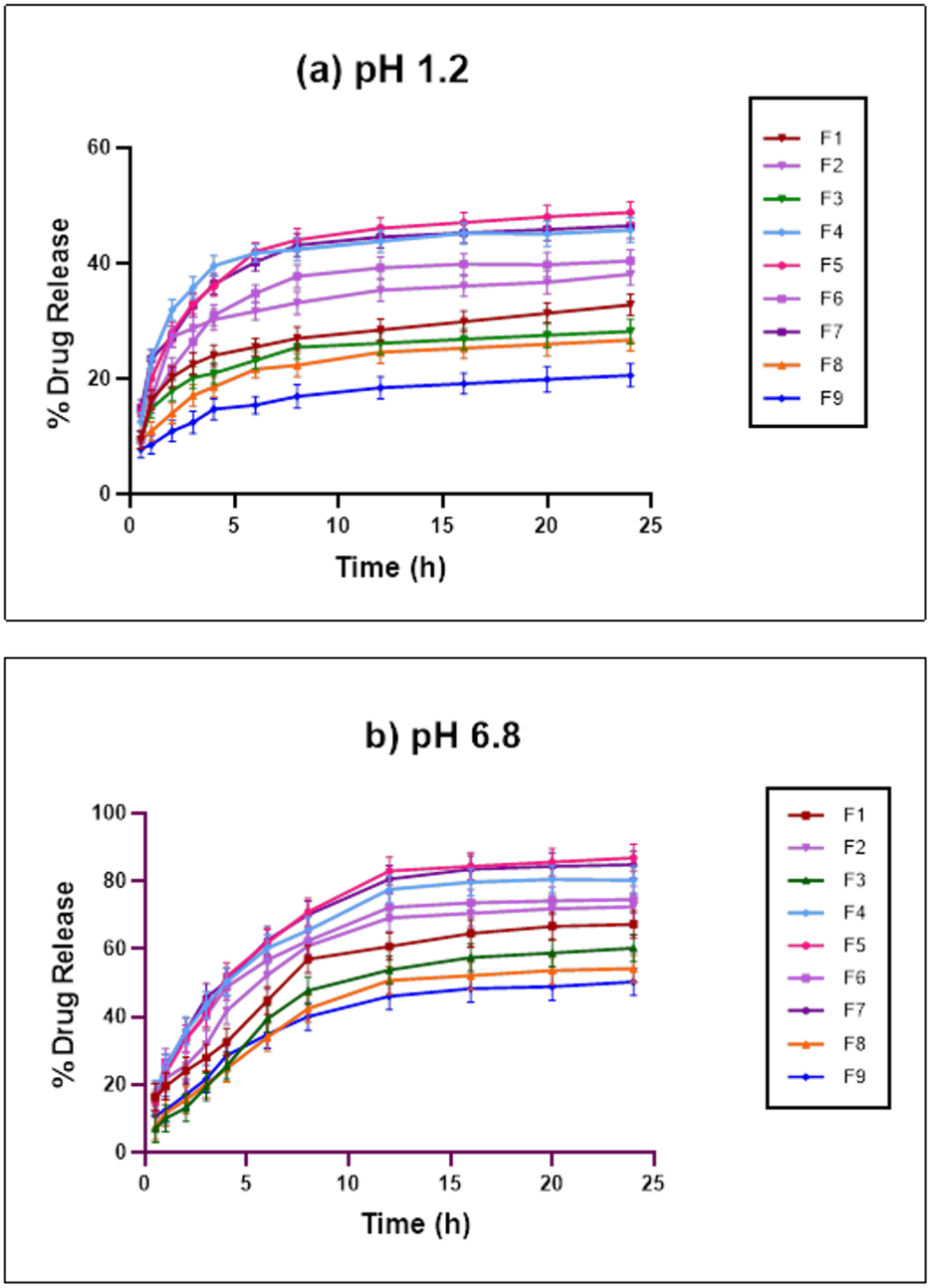

FIGURE 4.2: Percent drug release of formulations (F1 – F9) (a), SGF pH 1.2 (b), and SIF pH 6.8.

The in vitro drug release kinetics of the prepared TGR-loaded hydrogel formulations (F1–F9) were systematically investigated under simulated gastric (pH 1.2) and intestinal (pH 6.8) conditions using five established mathematical models, namely zero-order, first-order, Higuchi, Weibull, and Korsmeyer-Peppas, shown in

Table 4.2. The applicability of each model in describing the experimental release profiles was assessed based on the coefficient of determination (R^2) and statistical comparisons of model fitting using analysis of variance (ANOVA) of the residual sums of squares, followed by post-hoc testing.

Among these, the Korsmeyer-Peppas model consistently demonstrated the best fit, with R^2 values ranging from 0.8574 to 0.9956 at pH 1.2 and 0.9335 to 0.9901 at pH 6.8, alongside statistically significant differences in goodness-of-fit compared to each of the other individual models ($p < 0.001$). Furthermore, the release exponent (n) values obtained for these formulations were between 0.40 and 0.55 at pH 1.2 and 0.47 to 0.59 at pH 6.8 [103].

For hydrogel matrices exhibiting cylindrical geometries, n values exceeding 0.45 are indicative of anomalous (non-Fickian) transport mechanisms, wherein drug release is governed predominantly by a combination of Fickian diffusion and polymer chain relaxation or erosion. These findings suggest that drug release proceeds via a coupled process involving an initial swelling phase, driven by water penetration and polymer matrix relaxation, followed by diffusion of TGR through the hydrated polymer network [128]. The Higuchi model provided significantly better fits than the Weibull, zero-order, and first-order models ($p < 0.01$), with R^2 values ranging from 0.7438 to 0.9379 at pH 1.2 and 0.9122 to 0.9763 at pH 6.8, further supporting the presence of a substantial diffusion-controlled component within the overall release process.

In this case, TGR transport is primarily facilitated by concentration gradients established within the hydrated hydrogel matrix, consistent with classical Fickian diffusion principles. The Weibull model, being empirical in nature, exhibited variable fitting performance, with R^2 values ranging from 0.5202 to 0.7726 at pH 1.2 and 0.6935 to 0.7921 at pH 6.8. While certain formulations, such as F5 ($R^2 = 0.7921$) and F8 ($R^2 = 0.7769$) at pH 6.8, demonstrated the highest R^2 values within the Weibull model, the overall statistical comparison revealed significantly inferior fitting compared to both the Korsmeyer-Peppas and Higuchi models ($p < 0.05$), suggesting the limited mechanistic insight provided by this empirical approach. The zero-order model, which theoretically describes ideal

constant release kinetics, exhibited moderate R^2 values ranging from 0.5776 to 0.8142 at pH 1.2 and 0.7311 to 0.8986 at pH 6.8, with statistically significant differences in goodness-of-fit relative to the Korsmeyer-Peppas model ($p < 0.001$), indicating that complete zero-order release behavior was not achieved. The first-order model demonstrated the poorest fit among all models tested, with R^2 values ranging from 0.2301 to 0.3295 at pH 1.2 and 0.2975 to 0.4987 at pH 6.8, and these differences were confirmed as statistically significant ($p < 0.001$), clearly indicating that the drug release process is largely independent of the remaining TGR concentration within the matrix. Collectively, these results unequivocally demonstrate that TGR release from the developed hydrogel matrices is governed predominantly by anomalous transport mechanisms, characterized by a synergistic interplay between polymer swelling, chain relaxation, and drug diffusion through the hydrated network. The pronounced hydrophilic nature of the polymeric constituents facilitates rapid water absorption, leading to matrix expansion and polymer disentanglement, which in turn enhances both polymer relaxation and diffusion-mediated TGR transport. These findings are in close agreement with previous reports on hydrophilic polymer-based hydrogel systems, wherein swelling-induced matrix modifications and complex non-Fickian release behavior constitute the primary mechanisms governing drug release profiles [128].

TABLE 4.2: Drug Release Kinetics Modeling of Drug-Loaded Hydrogels (F1-F9).

Sample Code	**pH**	Zero order kinetics **R^2**	First order kinetics **R^2**	Higuchi model **R^2**	Weibull Model **R^2**	Korsmeyer-Peppas Model **R^2**	**n**
F1	1.2	0.7236	0.2495	0.8461	0.7689	0.9956	0.45
	6.8	0.7971	0.3372	0.9249	0.7005	0.973	0.5
F2	1.2	0.5776	0.2301	0.7438	0.5202	0.9918	0.4
	6.8	0.7311	0.2975	0.9122	0.6981	0.9789	0.47
F3	1.2	0.8142	0.3295	0.9379	0.7206	0.9629	0.45
	6.8	0.8601	0.4056	0.9589	0.7335	0.9774	0.49
F4	1.2	0.6187	0.2588	0.858	0.6258	0.9417	0.46
	6.8	0.8022	0.3358	0.9235	0.6935	0.9335	0.59
F5	1.2	0.7159	0.2375	0.8595	0.7726	0.9925	0.55
	6.8	0.8707	0.3384	0.9691	0.7921	0.9901	0.56

Table 4.2 continued from previous page

Sample Code	pH	Zero order kinetics R^2	First order kinetics R^2	Higuchi model R^2	Weibull Model R^2	Korsmeyer-Peppas Model R^2	n
F6	1.2	0.6679	0.2385	0.8408	0.576	0.9168	0.49
	6.8	0.8594	0.437	0.962	0.7702	0.9845	0.51
F7	1.2	0.6971	0.2461	0.8492	0.7102	0.955	0.52
	6.8	0.8986	0.4987	0.9763	0.7498	0.9825	0.533
F8	1.2	0.6365	0.2735	0.8115	0.5635	0.8574	0.48
	6.8	0.8373	0.3794	0.9596	0.7769	0.9753	0.47
F9	1.2	0.7695	0.3065	0.9106	0.5772	0.9604	0.53
	6.8	0.8404	0.4479	0.9452	0.7273	0.9775	0.55

4.3 Swelling Study

4.3.1 Effect of pH

The systematic study was carried out to explore the potential of intestinal-targeted delivery of hydrogel formulations (F1-1F9) by assessing the pH-dependent swelling response of hydrogel formulations under physiological condition simulations. Figure 4.3 shows an overall trend observed in all formulations to show a very high swelling ratio in simulated intestinal fluid (SIF, pH 6.8) than the simulated gastric fluid (SGF, pH 1.2), and this variation with pH was found to be statistically significant (paired t-test, $p = 0.0029$, $p < 0.05$). The formulations with the highest swelling ratio were formulation F5, which consists of 1% carboxymethyl cellulose (CMC), 6% xanthan gum (XG), and 4% acrylic acid (AA) with a swelling ratio of 12.41 ± 0.20 at pH 6.8, followed by F7 that contained 12% AA with a swelling ratio of 11.33 ± 0.25 and F4 that had 4% XG (10.38 ± 0.13). These findings are clear indicators that increments of ionizable polymers, e.g., XG, AA increases the swelling capacity of hydrogels in basic environments. By contrast, the formulation F9 that had the highest concentration of crosslinkers (0.7% N,N-methylenebisacrylamide, MBA) showed the lowest swelling (3.60 ± 0.16 at pH 6.8), which is 48.5% lower than that of the base formulation F1 containing 0.3% MBA. The given pH-dependent swelling behavior is attributed to the transition

of ionization in the hydrogel structure. At intestinal pH (6.8), carboxylic acid groups (-COOH) contained in AA and XG are deprotonated to form negatively charged carboxylate anions (-COO-), which cause electrostatic repulsion between the polymer chains in the network leading to swelling and facilitate uptake of water [129]. This process is further enhanced by deprotonation of pyruvyl (-CO-CH_3) and O-acetyl (-$OCOCH_3$) functional groups included in XG at pH greater than 6.0, which contribute to increasing charge density and hydrophilicity of the network [130]. However, at gastric pH (pH 1.2), these functional groups remain mainly protonated, resulting in a lower degree of ionization and negatively charged functional groups repelling, giving rise to a condensed network structure and reduced swelling [131].

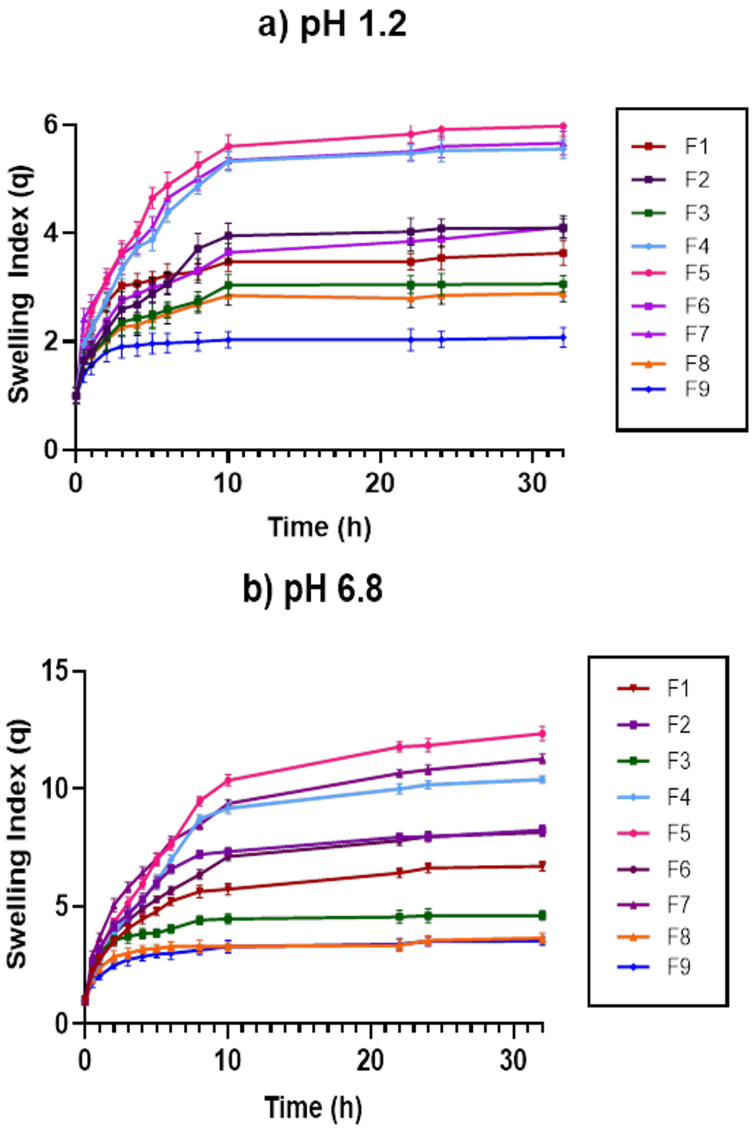

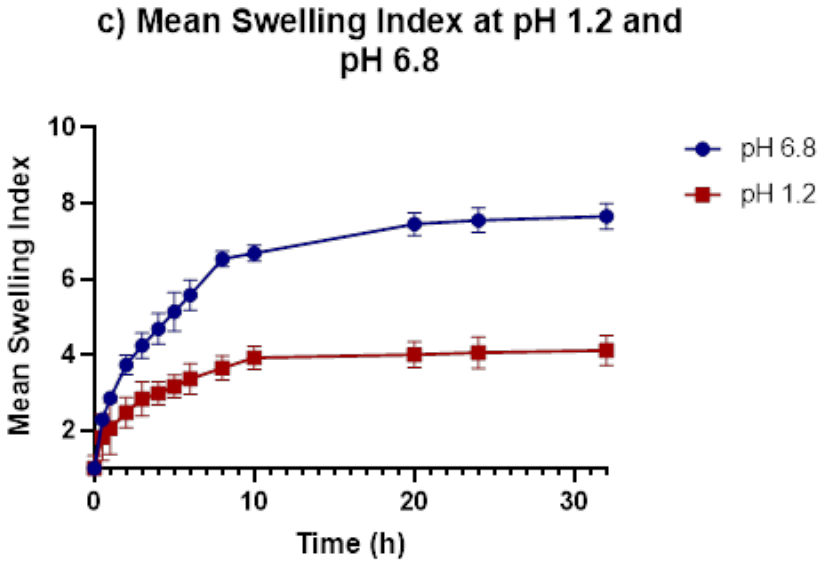

FIGURE 4.3: Swelling index of TGR-loaded Formulations (a), at pH 1.2 (b), at pH 6.8 (c), mean swelling Index.

Formulation composition analysis showed well-defined structure-function relationships to govern swelling behavior. As the XG concentration went up (2 to 6 percent XG; F1 and F5), there was a 77.5% increment in swelling at pH 6.8, attributable to a higher accessibility of hydrophilic, ionizable moieties along the matrix. Likewise, it was also observed that raising the AA content up to 12% (F7) raised the swell by 62.1% due to the increase in the anionic charge density that leads to the expansion of the network. Conversely, an increase in CMC content (1% F1 and 3% F3) led to a 33.9% reduction in swelling, possibly by creating steric hindrance between non-ionizable chains of cellulose, hence hindering network relaxation. Additionally, higher crosslink density, which was achieved by increasing MBA concentration from 0.3% (F1) to 0.7% (F9), caused a 48.5% reduction in polymer against available bonds (72.1% against 120.6%), as reflected by the decrease in swelling; thus, showing that by increasing the density of crosslinks, physical restriction of polymer chain movements and solvent infiltration inhibits swelling. All these findings indicate that the swelling characteristics of the formed hydrogels can be accurately tuned based on the concentration of XG, AA, and MBA and are considered a rational design scheme towards the pH sensitivity required in site-specific, intestinally targeted drug delivery.

4.3.2 Effect of Reactant Composition on Swelling

4.3.2.1 Effect of polymers

The effect of different polymer concentrations to the swelling behavior of the fabricated hydrogels was systematically studied. A swelling ratio was significantly increased when the concentration of the xanthan gum (XG) was increased to 6 g, as shown in Figure 4.4.

In particular, F5 (6 g XG) showed the best swelling capacity, then F4 (4 g XG) and F1 (2 g XG), and the trend of their swelling capacities is represented as F5 > F4 > F1. This tendency is explained by the presence of higher hydrophilicity due to higher XG content, because XG possesses increases the density of hydroxyl (-OH) groups in the polymeric network F1 [132]. These hydrophilic moieties, coupled with electrostatic repulsion between ionized carboxylate groups in a basic medium, contribute to the expansion of these networks and facilitate greater water uptake [90].

Statistical analysis confirmed a significant difference in swelling index across the varying XG concentrations ($p < 0.001$).

Similarly, carboxymethyl cellulose (CMC) concentration effects on swelling behavior were examined. One-way ANOVA indicated that there is a statistically significant difference between the formulations containing different content of CMC (F1-F3, $p < 0.05$).

The extent of swelling of hydrogel was also found to be coupled with the accessibility of hydrophilic carboxyl (-COOH) sites in the network. Remarkably, the F3, which had the highest concentration of CMC, portrayed a reduction in the swelling. This decrease is explained by higher density of crosslinking at elevated CMC content that limits the entrance of free water into the hydrogel matrix.

Therefore, the available space to absorb water into the network is restricted by the too extensive crosslinking of the, reaction and always leads to the reduced swelling capacity under all types of parameters in testing [133].

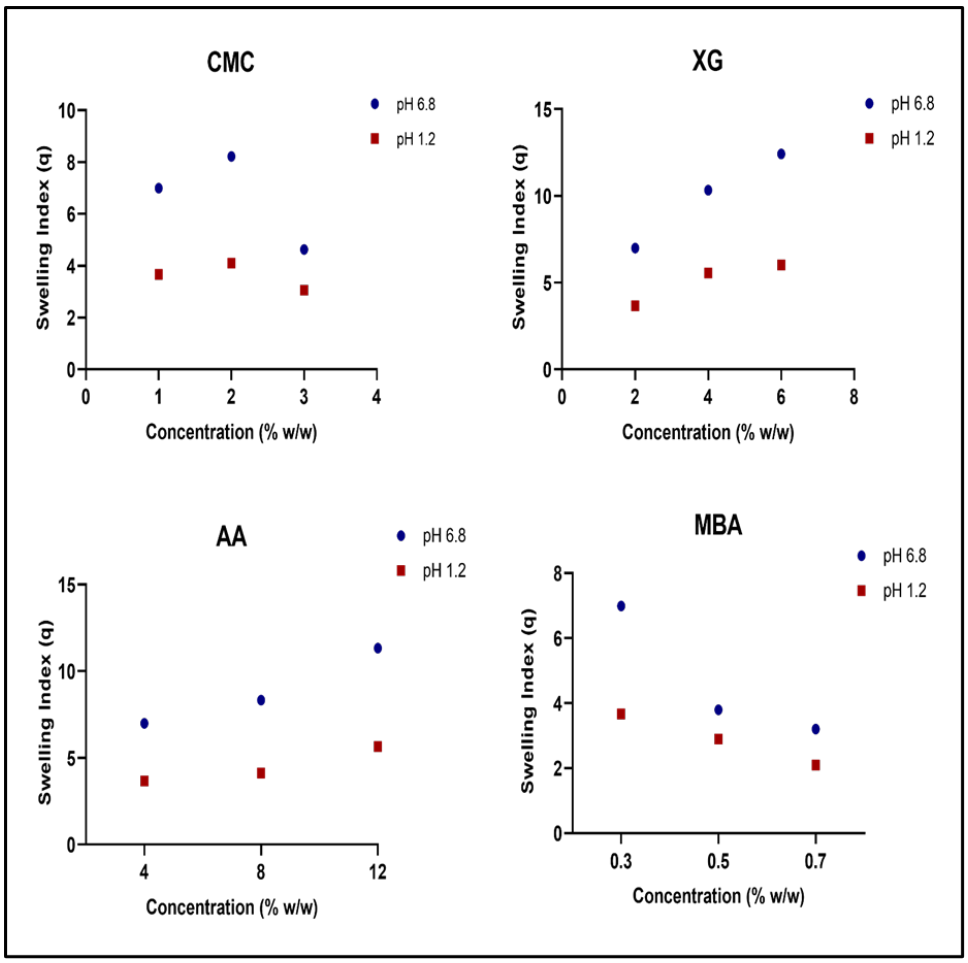

FIGURE 4.4: Influence of % w/w of CMC, AA, XG, and MBA on swelling index of TGR-loaded hydrogel.

4.3.2.2 Effect of Monomer

The effect of acrylic acid (AA) concentration on the swelling behavior of the fabricated hydrogels was methodically determined. Other formulation variables were held constant, and the level of AA was varied. As shown in Figure 4.4, as the concentration of AA increased in an incremental manner, a corresponding increase in the swelling ratio of the hydrogels was observed as well, with F7 > F6 > F1. Such is the character of the intrinsic pKa of AA, which is less than 4.2. Below pH 4 (acidic condition), maximum electrostatic repulsion between carboxylic groups of AA is not formed in the polymeric network, and therefore, the resulting swelling is restricted [134]. Ionization of carboxyl groups, however, takes place under neutral to slightly alkaline conditions (pH 6-8) producing negatively charged carboxylate

ions. Such ionization causes an electrostatic interaction of repelling forces between the polymer chains, leading to significant network expansion and improved water uptake, which ultimately facilitates effective swelling and drug release [135].

The findings established that there was a strong statistical correlation between AA concentration and swelling index ($p < 0.0001$) and the crucial effect of AA content in controlling the swelling behavior of the hydrogel system. Formulation F7 having 12 g of AA, was the formulation that showed the maximum swelling amongst the various tested formulations. In contrast, the swelling and release of drugs were lower at acidic pH as a result of the predominance of non-dissociated carboxylic groups and stable hydrogen associations between AA and the polymer matrix restricting network swelling [89].

4.3.2.3 Effect of Crosslinker

N,N,methylenebisacrylamide (MBA), the cross-linking agent, controls the three-dimensional network formation by covalently cross-linking functional groups of the polymer chains. Statistical analysis showed a strong quadratic regression between MBA concentration and swelling index ($p < 0.0001$, polynomial regression). Figure 4.4 demonstrated that an optimal MBA concentration (0.3 g in F1) provided the highest network efficiency, giving maximum swelling (6.99 ± 0.18) and gelation by balanced crosslinking. Further increase in formulations F8 (0.5 g MBA; 3.72 ± 0.21) and F9 (0.7 g MBA; 3.60 ± 0.16) demonstrated significant decreases in swelling capacity (Tukey post-hoc: $p<0.001$ vs F1), up to 47% and 48%, respectively.

The cause of this inverted relationship is the over-crosslinked network [136], which causes a decrease in the average mesh size (12.3 nm F1 to 12.3 nm- F9) using Flory-Rehner calculations. The ensuing network stiffness limits the mobility and water move-ability in the chain and reduces the equilibrium water absorption by more than 40% at physiologic pH. Consequently, swelling entropy is substantially diminished despite complete gelation, demonstrating the critical balance between structural integrity and functional expandability [137]. After thorough statistical

analysis of the efficiency of the drug entrapment, the kinetics of the swelling, and the release profile of the drugs, formulation F5 was selected for further characterization.

4.4 Fourier Transform Infrared Spectroscopy

The structural characteristics of TGR, the polymeric excipients (xanthan gum, XG; carboxymethyl cellulose, CMC; acrylic acid, AA), and the resultant TGR-loaded hydrogel system were investigated using Fourier Transform Infrared (FTIR) spectroscopy, as depicted in Figure 4.5.

The spectrum of XG exhibited characteristic vibrational modes indicative of its polysaccharide structure: a broad peak at 3284 cm^{-1} attributed to H-bonded O-H stretching, C-H stretching at 2895 cm^{-1}, ester carbonyl (C=O) stretching at 1726 cm^{-1}, the asymmetric stretch of the pyruvate carboxylate group (COO^-) at 1600 cm^{-1}, C-H bending at 1417 cm^{-1}, and C-O stretching of primary alcohols at 1020 cm^{-1}. Further confirmation of its polysaccharide nature was provided by prominent absorptions within the 920–1100 cm^{-1} region, assigned to C-O and C-C stretching vibrations [138].

The FTIR spectrum of TGR revealed defining functional groups: N-H and O-H stretching vibrations at 3380 and 3290.61 cm^{-1}, aliphatic C-H stretching at 2911.63 cm^{-1}, N-H bending modes at 1610.58 cm^{-1} and 1520 cm^{-1}, methyl bending at 1430 cm^{-1}, C-OH stretching at 1217.35 cm^{-1}, and C-O stretching vibrations at 1102 and 1075 cm^{-1} [139].

Acrylic acid (AA) displayed a broad hydroxyl (O-H) stretch at 3071 cm^{-1}, the characteristic carbonyl (C=O) stretch of the carboxylic acid group at 1700 cm^{-1}, and C=C stretching at 1611 cm^{-1} [140].

The CMC spectrum featured key peaks corresponding to O-H stretching influenced by intermolecular and intramolecular hydrogen bonding at 3263 cm^{-1}, anti-symmetrical C-H stretching at 2906 cm^{-1}, and asymmetric (1600 cm^{-1}) and symmetric (1415 cm^{-1}) stretching vibrations of the carboxylate anion (COO^-) [141].

Analysis of the TGR-loaded hydrogel system confirmed the successful integration of all components (CMC, XG, AA, TGR) into the formulation.

A broad, intense absorption band spanning 3200–3672 cm^{-1} was observed, corresponding to overlapping O-H stretching vibrations primarily from the hydrophilic polymers (XG, CMC, AA), signifying extensive hydrogen bonding within the polymeric network.

Critically, the persistence of characteristic TGR peaks at 3380 cm^{-1}, 3290.61 cm^{-1}, 1610.58 cm^{-1}, 1512 cm^{-1}, 1417 cm^{-1}, 1197 cm^{-1}, and 1057 cm^{-1} within the composite spectrum affirms the absence of significant chemical interaction between the drug and the polymeric matrix, suggesting TGR's structural integrity was maintained upon encapsulation.

The region between 1615 cm^{-1} and 1717 cm^{-1} contained complex C=O stretching vibrations, encompassing contributions from the carboxylate groups of CMC, the carboxylic acid/carboxylate functionalities of AA, and carbonyl groups inherent to TGR.

Peaks within 920–1100 cm^{-1} were consistent with C-O and C-C stretching modes of polysaccharide glycosidic linkages, predominantly originating from XG. Crucially, evidence for covalent crosslinking within the hydrogel network was provided by a discernible shift in the carbonyl stretching frequency associated with the acrylic acid monomer.

The characteristic C=O stretch of pure AA at 1700 cm^{-1}, indicative of the carboxylic acid (COOH) group, shifted to 1717 cm^{-1} in the crosslinked hydrogel formulation.

This shift is diagnostic of the conversion of carboxylic acid groups into ester linkages (COOR) during the crosslinking reaction, thereby confirming the formation of ester bonds between the polymeric components (CMC, XG) and the acrylic acid monomer.

This covalent crosslinking is fundamental to establishing the stable three-dimensional network structure essential for the hydrogel's functionality.

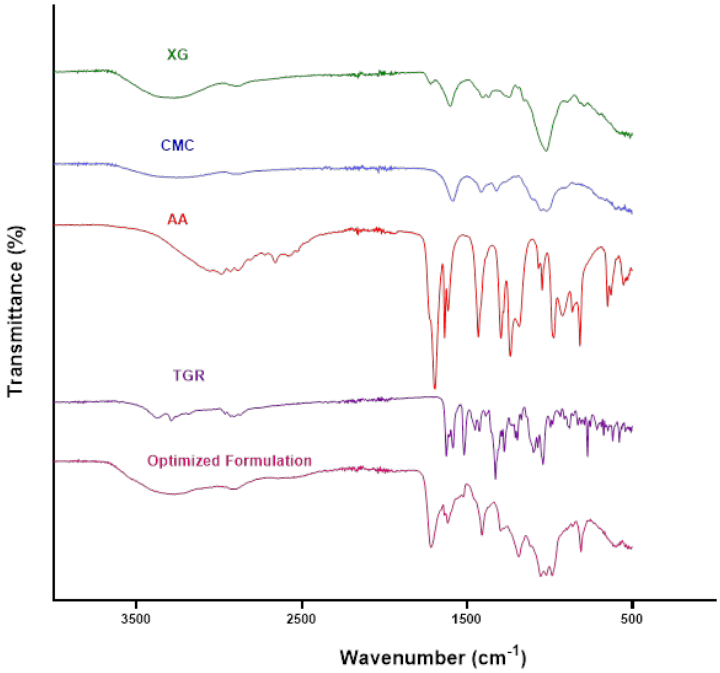

FIGURE 4.5: FTIR spectra of XG, CMC, AA, drug (TGR), and drug-loaded formulation.

4.5 Powder X-Ray Diffraction

The crystallinity and structural organization of carboxymethyl cellulose (CMC), xanthan gum (XG), pure drug (TGR), unloaded hydrogel, and drug-loaded hydrogel were comprehensively evaluated through powder X-ray diffraction (PXRD) analysis, as depicted in Figure 4.6.

The PXRD pattern of pure TGR exhibited well-defined and sharp diffraction peaks at 2θ values of 12.3^o, 17.7^o, 20.6^o, and 23.6^o, confirming its highly crystalline nature. These distinct peaks reflect the long-range molecular ordering and rigid lattice structure inherent to the crystalline drug substance, in agreement with previously reported data [106].

In contrast, XG displayed broad and diffuse halos with characteristic peaks at approximately $2\theta = 20.3^o$ and 28.9^o, indicative of its largely amorphous structure. The absence of sharp diffraction signals and the presence of a broad amorphous

halo suggest a lack of long-range order, which is typical for polysaccharides such as XG [142].

The diffraction pattern of CMC revealed a broad peak centered at $2\theta \approx 21^o$, accompanied by a minor peak at $2\theta \approx 10.09^o$. The presence of a peak around $2\theta = 10^o$ is characteristic of semi-crystalline domains within the CMC structure, commonly attributed to the specific degree of substitution and hydration state of the polymer, consistent with literature reports.

The broad nature of the peak at 21^o further confirms the predominantly amorphous nature of the CMC employed [33, 143].

The unloaded hydrogel exhibited a diffuse and broad diffraction pattern with no sharp peaks, characteristic of an amorphous three-dimensional polymeric network. This amorphous nature is desirable for hydrogel-based drug delivery systems, as it facilitates uniform drug dispersion and enhances matrix swelling behavior.

Notably, the PXRD pattern of the drug-loaded hydrogel demonstrated a significant attenuation of the characteristic crystalline peaks of TGR, with only faint traces of the original diffraction signals observed.

The substantial reduction in peak intensity, coupled with the absence of well-defined crystalline reflections, indicates a marked decrease in the crystallinity of the encapsulated drug.

This transformation from a crystalline to a partially amorphous state is attributed to the molecular entrapment and homogeneous dispersion of TGR within the hydrogel matrix. Such amorphization is known to improve the apparent solubility and dissolution profile of poorly water-soluble drugs, thereby enhancing their bioavailability.

Collectively, the PXRD data confirms the successful incorporation of TGR into the hydrogel system, with a concomitant reduction in crystallinity, supporting the potential of the formulated hydrogel as an effective carrier for controlled drug delivery.

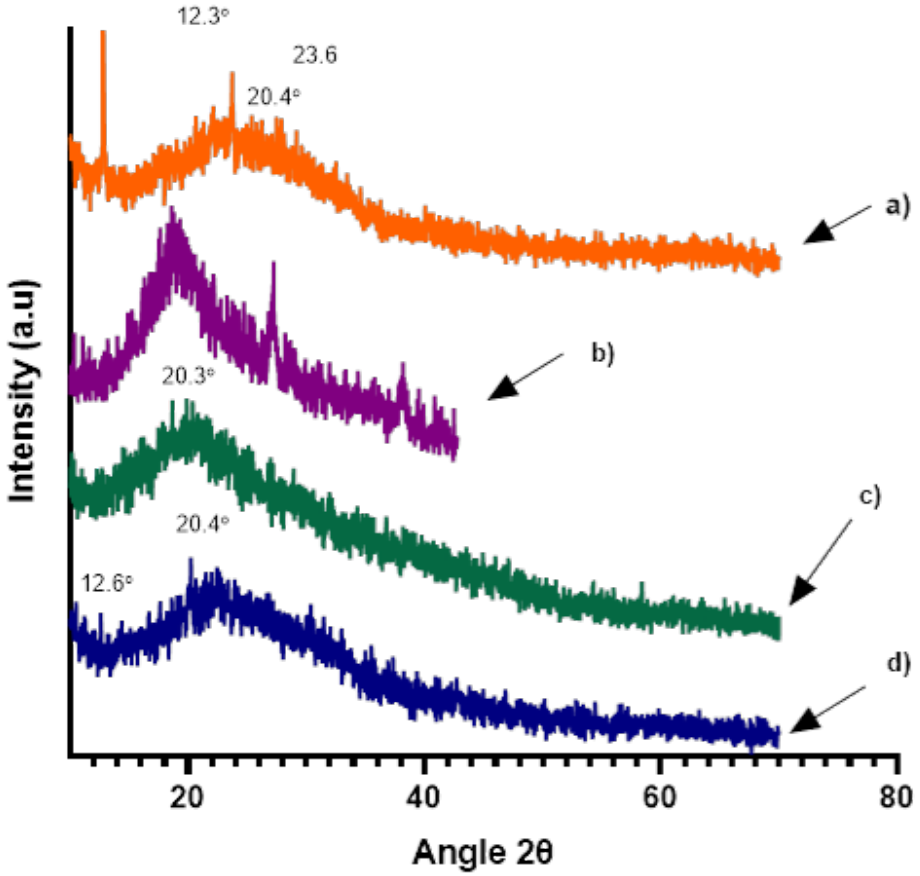

FIGURE 4.6: Powder X-ray diffraction patterns of a) TGR, b) CMC, c) XG, and d) TGR- loaded formulation.

4.6 Thermal Stability Analysis

The thermal stability and decomposition behavior of XG, CMC, pure drug (TGR), unloaded hydrogel, and drug-loaded hydrogel were systematically evaluated using thermogravimetric analysis (TGA), as illustrated in Figure 4.7.

The TGA thermogram of pure XG demonstrated high thermal stability, with an initial weight loss of approximately 14%, attributed to the evaporation of adsorbed moisture and volatile components below 100^{o}C. A two-step decomposition process was observed, wherein the first major weight loss occurred between 212^{o}C and 299^{o}C, followed by a significant degradation phase from 325^{o}C to 547^{o}C, resulting in an overall mass reduction of approximately 81% [144]. These findings are

consistent with the known decomposition behavior of polysaccharides, involving cleavage of glycosidic linkages and breakdown of the polymer backbone [145].

The thermogram of TGR exhibited minimal weight loss (∼3%) up to 241^{o}C, primarily due to residual moisture evaporation. A pronounced degradation phase was observed between 241^{o}C and 500^{o}C, corresponding to the thermal decomposition of the crystalline drug structure, with an overall mass loss of approximately 53% [146].

For CMC, an initial weight loss of 10–15% was recorded between 30^{o}C and 120^{o}C, attributed to moisture release. A prominent degradation event occurred between 230^{o}C and 350^{o}C, associated with the breakdown of the cellulose backbone and the decomposition of carboxymethyl functional groups, resulting in a total mass loss of approximately 40–50%. Residual char formation of approximately 30% at 500^{o}C reflects partial carbonization of the polymer matrix, consistent with previous literature reports [147, 148].

The unloaded hydrogel exhibited an initial weight loss below 100^{o}C, primarily due to moisture evaporation. Subsequent weight loss between 200^{o}C and 350^{o}C reflected the thermal degradation of the polymeric network. The relatively lower residual mass compared to the loaded hydrogel indicated reduced structural integrity and thermal stability.

In contrast, the drug-loaded hydrogel exhibited improved thermal stability, as evidenced by an initial 10–12% weight loss below 70^{o}C due to moisture evaporation, followed by a gradual degradation phase between 200^{o}C and 350^{o}C. This weight loss was attributed to the decomposition of polymeric components and partial drug transformation. Beyond 400^{o}C, further degradation was observed, likely corresponding to the breakdown of drug-polymer interactions and the complete degradation of the matrix. Notably, the drug-loaded hydrogel retained a higher residual mass compared to the unloaded formulation, indicative of enhanced thermal stability.

The improved thermal stability of the drug-loaded hydrogel is attributed to molecular-level interactions between the drug and polymer matrix, such as hydrogen bonding

and physical complexation, which restrict polymer chain mobility and delay the onset of degradation. These findings confirm the successful encapsulation of TGR within the hydrogel network and the formation of a structurally stable, thermally robust drug delivery system [149].

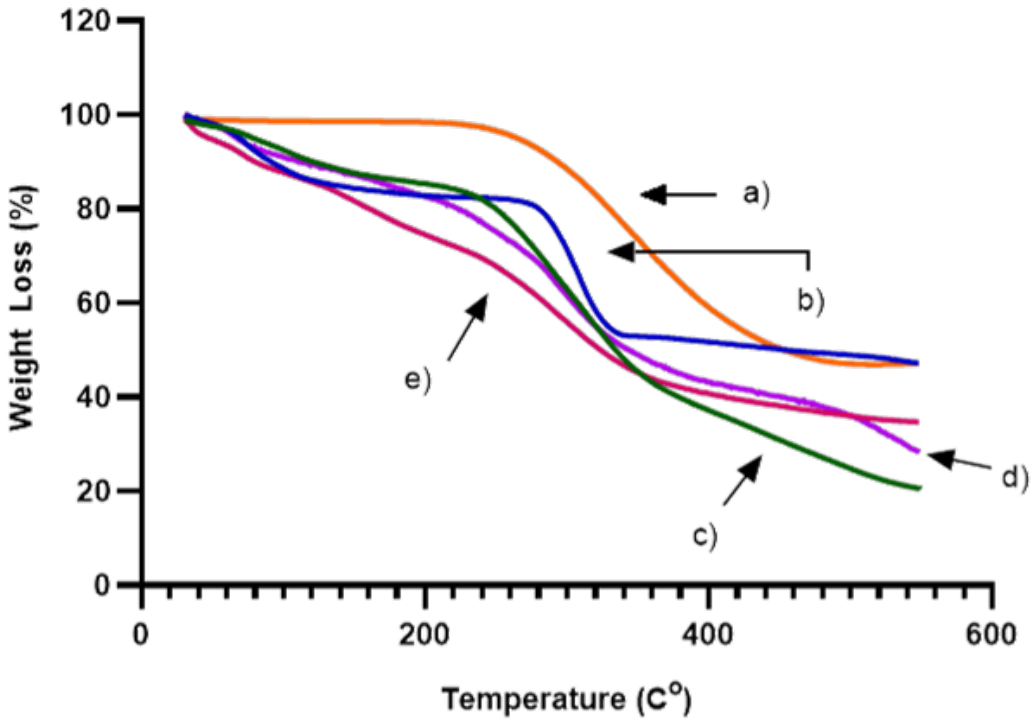

FIGURE 4.7: TGA thermograms (a) TGR, (b) CMC, (c)XG, (d) TGR-loaded hydrogel and (e) Unloaded hydrogel.

The thermal behavior and physical state of xanthan gum (XG), carboxymethyl cellulose (CMC), pure drug (TGR), unloaded hydrogel, and drug-loaded hydrogel were systematically investigated using differential scanning calorimetry (DSC), as shown in Figure 4.8.

The DSC thermogram of pure XG exhibited a broad endothermic peak centered around 84°C, attributed to the evaporation of adsorbed moisture. The absence of a distinct melting transition further confirmed the amorphous nature of XG, consistent with its polysaccharide structure. An onset of thermal degradation was observed at approximately 233.97°C, corresponding to polymer backbone decomposition, in agreement with reported literature on XG thermal degradation [150].

The thermogram of CMC revealed an initial endothermic event between 60^{o}C and 90^{o}C, associated with moisture loss.

Minor thermal transitions beyond 222^{o}C were observed, likely arising from structural rearrangements and partial degradation of the polymer. These thermal characteristics reflect the semi-crystalline nature of CMC, influenced by its degree of substitution and hydration state [151].

The DSC thermogram of pure TGR exhibited a sharp endothermic peak at approximately 140^{o}C, confirming its crystalline nature and characteristic melting point. Additionally, a distinct exothermic peak at 332^{o}C was observed, corresponding to drug decomposition and phase transition processes.

The unloaded hydrogel exhibited a broad, low-intensity endothermic peak, primarily corresponding to the release of loosely bound water. The absence of sharp transitions in the thermogram is indicative of an amorphous, crosslinked hydrogel matrix, wherein polymer network interactions mask distinct thermal transitions.

In contrast, the DSC thermogram of the drug-loaded hydrogel did not display the characteristic melting peak of TGR at 140^{o}C, nor the exothermic decomposition peak at 332^{o}C. The complete disappearance of these drug-specific thermal events suggests the successful molecular dispersion of TGR within the hydrogel matrix and a significant reduction in crystallinity.

This transition of the drug from a crystalline to an amorphous or molecularly dispersed state is a desirable outcome for enhancing drug solubility and bioavailability.

Furthermore, the absence of the drug melting peak indicates strong intermolecular interactions, such as hydrogen bonding, between the drug and the polymeric matrix, contributing to the overall thermal stability of the developed formulation [152].

Collectively, the DSC results confirm the effective encapsulation of TGR within the hydrogel, leading to amorphization of the drug and the formation of a thermally stable polymeric network suitable for controlled drug delivery applications.

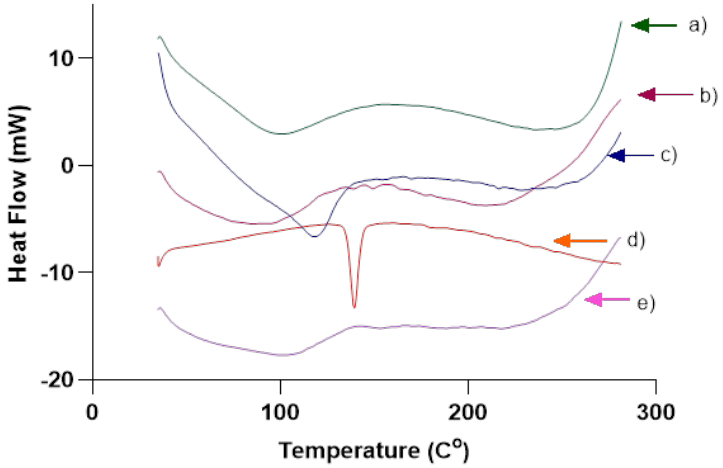

FIGURE 4.8: TGA thermograms (a) TGR, (b) CMC, (c) XG, (d) TGR-loaded hydrogel and (e) Unloaded hydrogel.

4.7 Scanning Electron Microscopy

The surface representation and the microstructural attributes of the lyophilized-hydrogel samples were thoroughly analyzed through Scanning Electron Microscopy (SEM). Figure 4.9 shows the representative SEM micrographs at different magnifications. The images also show a geometrically intricate, three-dimensional, percolating microporous structure with a high level of spatial heterogeneity, a hallmark characteristic to the process of lyophilization [153]. Under low/intermediate objectives (500 X to 1.00 K X; WD: 8.0-8.5 mm; EHT: 20.00 kV; C 20x detector), the hydrogel showed asymmetric pore geometries with irregular and lobate boundaries as well as non-uniform pore size distribution. The porous diameters were quite different, and interlinked throats were of the order of 0.5 to 2.0 M, providing percolating diffusion routes essential to controlled drug release [154]. The nanoscale pitting and fibrils on the pore walls were also observed under high-magnification imaging, which helps to increase the huge specific surface area of the matrix. Local microstructural flaws, such as crumpling of the surface at strut intersections, minor cracks, were observed, which are mostly related to the sublimation of ice crystals raised when freeze-dried. Nevertheless, these artifacts did not affect the main structure of the network architecture. These microcracks,

although usually contained, can provide some initial burst release effect–effect that needs to be considered in optimization of the formulation [155]. Notably, minor charging artifacts manifested as localized brightness at higher magnifications, despite the application of a uniform 15 nm gold sputter coating, likely resulting from the inherent hydrophilicity of residual polymeric components.

The hierarchical porous structure is a determining factor in the regulation of the functional properties of the hydrogel. The high connectivity between the pores allows capillary driven immersion of water and an efficient rate of water uptake, which is key to drug loading and subsequent drug release. In addition, tortuous and heterogeneous diffusion pathways in the matrix permit longevity of diffusion-controlled release of therapeutic agents, which is the key requirement of developing tunable and responsive drug delivery systems. Ultimately, all of these microstructural characteristics highlight the prospects of the fabricated hydrogel system as a viable material ready to be advanced in controlled-release biomedical applications.

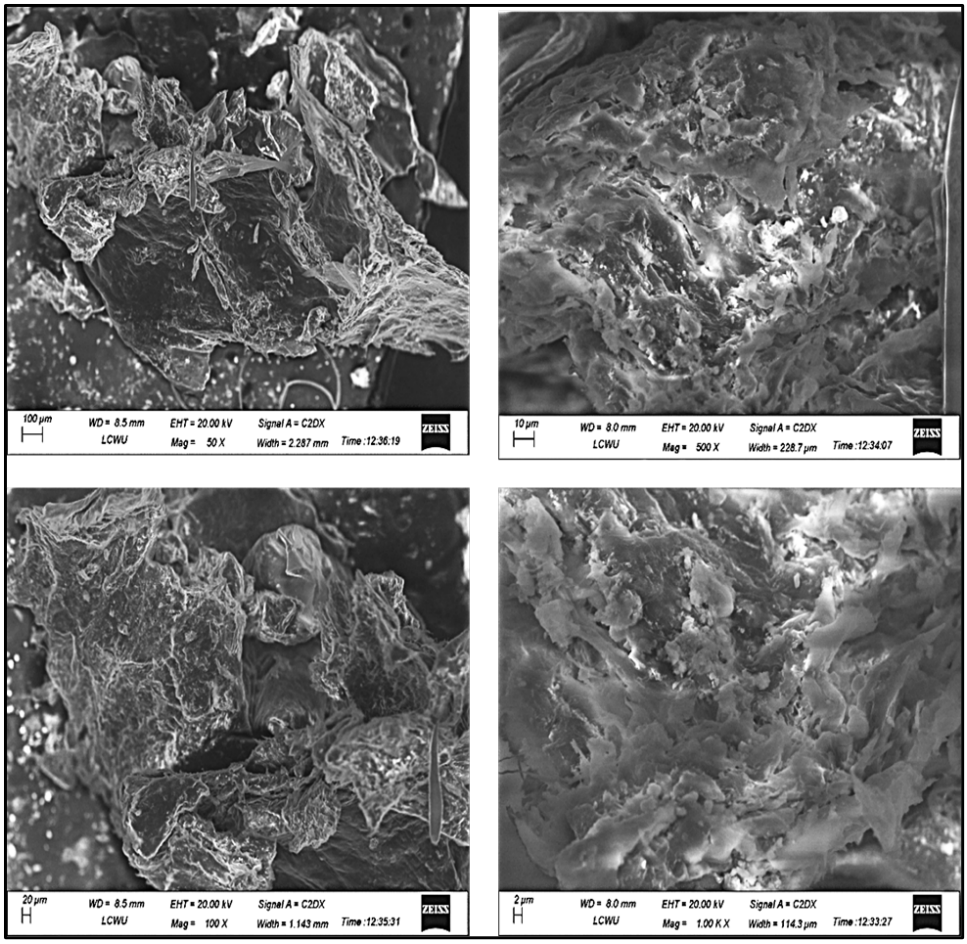

FIGURE 4.9: SEM Micrographs of CMC/XG Hydrogel.

4.8 Acute Oral Toxicity Studies

The biological safety and systemic tolerability of optimized hydrogel formulation (F5) were evaluated by conducting acute oral toxicity study followed by OECD Test Guideline 423. The treated group received the labelled F5 drug-loaded hydrogel to a single oral dose of 2 g/kg body weight and the control group was given the same amount of physiological saline. Clinical manifestation of toxicity, mortality, behavioral changes, and pool changes in body weight, food and water consumption and general appearance were evaluated during a 14-day observation period in all animals. During the whole observation, there were no deaths, and no evidence of any toxicity was observed in both groups. No abnormalities in behavioral responsiveness such as locomotor activity, grooming behavior, response to touch, corneal reflexes, and, most importantly, no manifestations of lethargy, tremors, convulsions, piloerection, salivation and gastro-intestinal distress (vomiting and diarrhea) were observed amongst the animals, as shown in Table 4.3. Both groups showed normal physiological pattern in body weight gain and maintained food and water intake, further suggesting no presence of a systemic toxicity [156].

Table 4.3: Clinical Observations.

Time	**Control Group**	**Experimental Group**
	Body Weight (g)	
Day 1	27.93 ± 2.5	29.23 ± 1.2
Day 7	29.38 ± 2.6	30 ± 0.5
Day 14	31 ± 2.0	32 ± 0.6
	Observation Parameters	
Mortality	−	−
Body weight changes	+	+
Locomotor activity	+	+
Grooming behavior	+	+
Food intake	+	+
Water intake	+	+
Salivation	−	−
Corneal response	+	+
Touch response	+	+
Convulsions/tremors	−	−
Lethargy	−	−

Note: + and – sign indicates presence and absence of specified observation, respectively.

At day 14, all the animals were euthanized by exsanguination to carry out the complete hematological, biochemical and histopathological analyses. Hematological findings, demonstrated in Table 4.4, indicated that all the parameters of red blood cell count, hemoglobin concentration, hematocrit, mean corpuscular volume, mean corpuscular hemoglobin, platelet count, and leukocyte differentials were found within the normal physiological limits in both groups, and there was no statistically significant variation ($p > 0.05$).

These outcomes demonstrate that the oral administration of the F5 hydrogel did not have an adverse impact on the hematopoiesis.

These outcomes demonstrate that the oral administration of the F5 hydrogel did not have an adverse impact on the hematopoiesis. Biochemical examination also indicated that there were no hepatic or renal toxicity, because major indicators such as serum urea, creatinine, alanine aminotransferase (ALT), aspartate aminotransferase (AST), alkaline phosphatase (ALP), albumin, triglycerides, bilirubin, cholesterol, and glucose concentrations were within physiological limits, and had no significant difference between treated and control animals ($p > 0.05$), as shown in Table 4.5 [157].

Histological analysis of vital organs such as the liver, kidneys, heart, lungs, spleen and stomach were the comparable as the control group, and showed no signs of degeneration of cells, inflammatory infiltrate, necrosis and any structural anomalies, as given in Figure 4.10 [104].

Combined with the insignificance of the hematological and biochemical data, the lack of microscopic lesions in organs accompanied by the good systemic biocompatibility of the F5 hydrogel formulation at the tested dose comprises the evidence of its excellent systemic biocompatibility.

Overall, clinical and hematological, biochemical and histopathological considerations confirmed the biological safety of the F5 hydrogel after an acute dose of oral administration, justifies further preclinical testing of the system as a controlled drug delivery system.

TABLE 4.4: Hematological Analysis.

Parameter	**Control Group (Mean ± SD)**	**Treated Group (Mean ± SD)**
WBC ($\times 10^3/\mu$L)	6.5 ± 0.6	7.1 ± 0.7
RBC ($\times 10^6/\mu$L)	7.8 ± 0.5	8.2 ± 0.4
Hb (g/dL)	14.2 ± 0.8	14.9 ± 0.6
HCT (%)	42.1 ± 2.4	44.3 ± 2.1
MCV (fL)	45.0 ± 1.8	50.2 ± 1.7
MCH (pg)	16.2 ± 1.1	16.7 ± 0.9
Platelets ($\times 10^3/\mu$L)	750 ± 65	709 ± 58
Lymphocytes (%)	75.4 ± 3.5	78.1 ± 4.0
Neutrophils (%)	20.7 ± 2.9	19.4 ± 2.7
Eosinophils (%)	2.81 ± 0.8	1.8 ± 0.4

TABLE 4.5: Biochemical Blood Analysis.

Parameters	**Control Group (Mean ± SD)**	**Treated Group (Mean ± SD)**
Urea (mg/dL)	44.5 ± 3.2	47.7 ± 2.8
Creatinine (mg/dL)	0.4 ± 0.06	0.6 ± 0.04
ALT (U/L)	54.2 ± 4.1	58.7 ± 3.6
AST (U/L)	121.5 ± 5.3	130.2 ± 4.9
ALP (U/L)	98.4 ± 6.7	85.3 ± 7.1
Albumin	3.8 ± 0.3	4.0 ± 0.2
TG (mg/dL)	90.5 ± 7.8	94.3 ± 6.5
Bilirubin (mg/dL)	0.8 ± 0.1	0.6 ± 0.08
Cholesterol (mg/dL)	155.6 ± 12.3	142.4 ± 11.7
Glucose (mg/dL)	120.2 ± 10.1	110.5 ± 9.4

Note: Data expressed as Mean ± SD (n = 5). Statistical analysis performed using Student's t-test; $p > 0.05$ indicates no significant difference

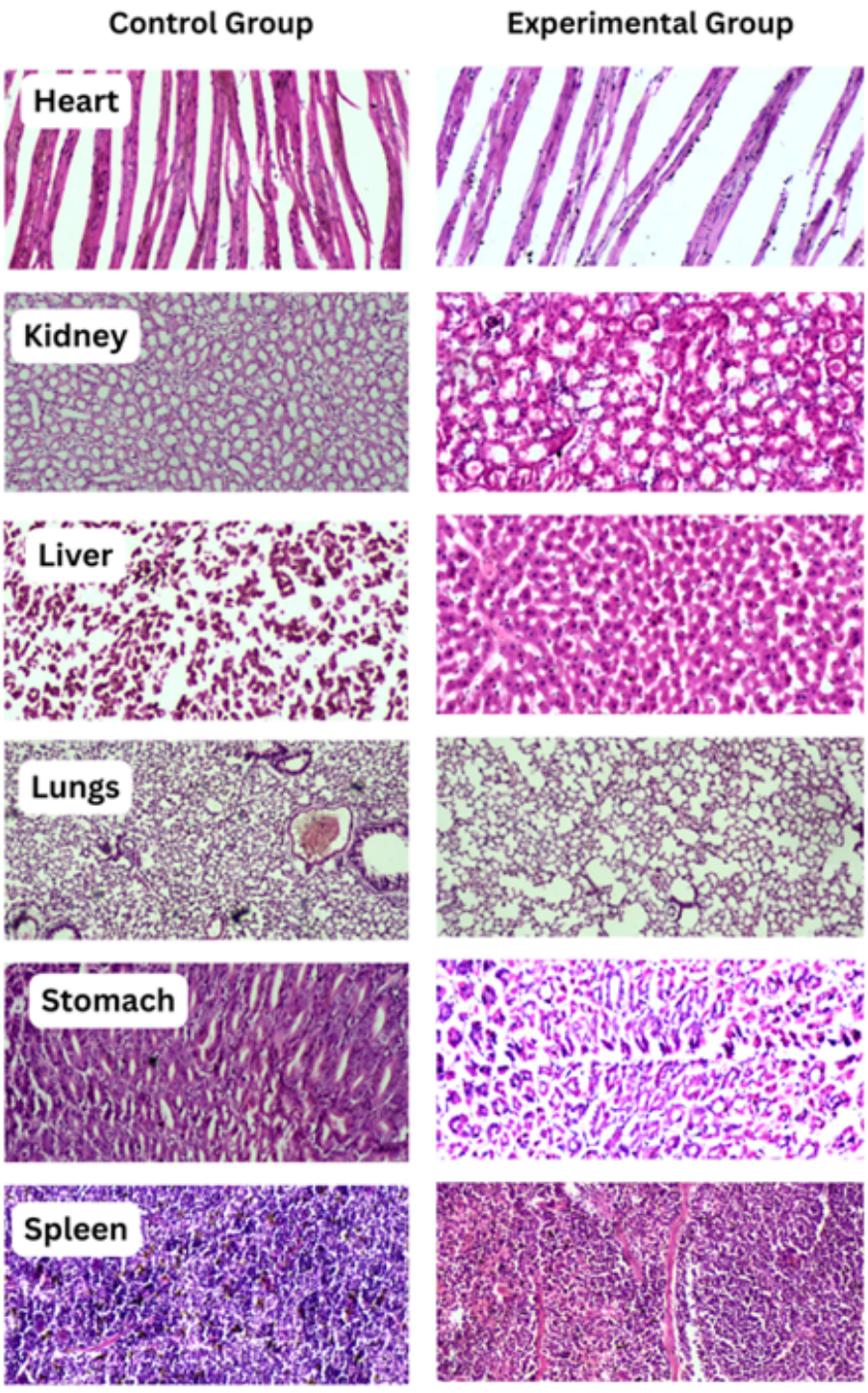

FIGURE 4.10: Histological assessment of vital organs control and experiment groups.

Chapter 5

Conclusion and Recommendations

5.1 Conclusion

This study successfully engineered a pH-responsive interpenetrating polymer network hydrogel composed of xanthan gum, carboxymethyl cellulose, and acrylic acid for targeted oral delivery of TGR. Comprehensive characterization confirmed covalent crosslinking through FTIR analysis (ester bond formation at 1717 cm^{-1}), ensuring physical drug entrapment without chemical degradation, while thermal studies (TGA/DSC) revealed enhanced matrix stability with degradation onset $>200^{o}$C. Critically, the hydrogel exhibited pH-dependent functionality, demonstrating a 2.41-fold higher equilibrium swelling ratio at intestinal pH 6.8 (13.02 $\pm$ 0.41) versus gastric pH 1.2 (5.41 $\pm$ 0.32; $p < 0.001$), which facilitated sustained drug release achieving 86.83 $\pm$ 0.45% cumulative delivery over 24 h through anomalous diffusion kinetics (Korsmeyer-Peppas n = 0.56). These properties directly address TGR's limitations as a BCS Class IV drug—low solubility (10–15 μg/mL) and bioavailability ($\approx$36%)—by protecting the drug from gastric degradation, enabling intestine-specific release, and providing zero-order kinetics suitable for once-daily dosing. Coupled with excellent acute safety profiles (OECD 423, 2

g/kg), this platform shows significant potential for clinical translation pending in vivo bioavailability validation.

5.2 Future Recommendations

The obtained pH-sensitive hydrogel formulation of TGR has exhibited encouraging in vitro properties; nevertheless, there are a number of important issues that should be considered in future studies. First, the performance of the hydrogel system needs confirmation in physiological conditions and should undergo significant in vivo pharmacokinetic and pharmacodynamic studies. The oral bioavailability, systemic circulation kinetics, targeted site release, and overall pharmacotherapy of TGR, when applied through this hydrogel matrix should be established in these studies.

Moreover, the toxicity and prolonged biocompatibility studies are required for sufficient data on safety and tolerance of the hydrogel system, or the adverse impacts that may be manifested with repeated administration. Since the formulation is administered orally, emphasis must be placed on the gastric compatibility of the formulation and potential mucosal interactions.

Moreover, real-time and accelerated stability testing should be performed according to ICH recommendations in order to determine the shelf life and storage conditions of the final product. Such studies will assist in the viability of a usable dosage form that can prevail through fluctuating environmental conditions in the transportation and storage process.

Another area of future research could focus on **modifying the hydrogel network** to allow for **dual or multi-drug loading**, potentially enabling combination therapy strategies. This could involve co-delivery of TGR with other antiplatelet agents, anticoagulants, or drugs that improve cardiovascular outcomes. The synergistic effects of such combinations could be studied to determine whether lower doses can be used without compromising therapeutic outcomes, thereby reducing the risk of side effects.

Moreover, investigation on possible modifications the surface of the hydrogel with targeting ligands, e.g. peptides or antibodies, could augment adhesion to the mucosa, achieve a site-specific delivery to the small intestine or the cardiovascular tissue. The design can also be modified to incorporate the multi-stimuli-responsive behavior where the hydrogel is responsive not only to pH but also to the enzyme or temperature variations that can further improve the delivery of the drugs in a controlled and targeted manner.

At the patient-centric level, this can be made by designing user-friendly dosage forms, e.g. orally disintegrating tablets containing hydrogel microspheres or, capsules containing hydrogel microspheres that can help to achieve improved patient adherence and acceptance, especially in the patient population of elderly, or children.

Lastly, clinical trials must be undertaken to validate the performance of a hydrogel system in human beings, and should conceptualize on how to promote the drug bioavailability, minimize its dosing interval, and develop patient compliance. Eventually, positive findings in the pre-clinical experiments are expected to provide the basis of clinical trial which is important to evaluate the safety, effectiveness, pharmacokinetics and the final therapeutic value of the hydrogel formulation in humans. Regulatory channels and scale-up production process ought to be analyzed as well to enable the eventual commercialization.

Bibliography

[1] Cardiovascular disease. https://www.who.int/health-topics/cardiovascular-diseases (Accessed: October, 2025)

[2] A. Timmis, D. Kazakiewicz, N. Townsend, R. Huculeci, V. Aboyans, and P. Vardas, "Global epidemiology of acute coronary syndromes," Nature Reviews Cardiology, vol. 20, no. 11, pp. 778-788, 2023.

[3] A. Srivastava, M. A. Khan, S. Bedi, and U. Bhandari, "A Review on Different Solubility Enhancement Techniques of Ticagrelor," International Journal of Pharmaceutical Investigation, vol. 13, no. 1, 2023.

[4] M. Fan et al., "Covalent and injectable chitosan-chondroitin sulfate hydrogels embedded with chitosan microspheres for drug delivery and tissue engineering," Materials Science and Engineering: C, vol. 71, pp. 67-74, 2017.

[5] Z. Liu, W. Toh, and T. Y. Ng, "Advances in mechanics of soft materials: A review of large deformation behavior of hydrogels," International Journal of Applied Mechanics, vol. 7, no. 05, p. 1530001, 2015.

[6] E. M. Ahmed, "Hydrogel: Preparation, characterization, and applications: A review," Journal of Advanced Research, vol. 6, no. 2, pp. 105-121, 2015/03/01/ 2015.

[7] Z. Zare-Akbari, H. Farhadnejad, B. Furughi-Nia, S. Abedin, M. Yadollahi, and M. Khorsand-Ghayeni, "PH-sensitive bionanocomposite hydrogel beads based on carboxymethyl cellulose/ZnO nanoparticle as drug carrier," International Journal of Biological Macromolecules, vol. 93, pp. 1317-1327, 2016/12/01/ 2016.

[8] A. M. Abdel Ghaffar, R. R. Radwan, and H. E. Ali, "Radiation Synthesis of Poly(Starch/Acrylic acid) pH Sensitive Hydrogel for Rutin Controlled Release," International Journal of Biological Macromolecules, vol. 92, pp. 957-964, 2016/11/01/ 2016.

[9] G. R. Mahdavinia, A. Mosallanezhad, M. Soleymani, and M. Sabzi, "Magnetic- and pH-responsive κ-carrageenan/chitosan complexes for controlled release of methotrexate anticancer drug," International Journal of Biological Macromolecules, vol. 97, pp. 209-217, 2017/04/01/ 2017.

[10] M. Yadollahi, S. Farhoudian, S. Barkhordari, I. Gholamali, H. Farhadnejad, and H. Motasadizadeh, "Facile synthesis of chitosan/ZnO bio-nanocomposite hydrogel beads as drug delivery systems," International Journal of Biological Macromolecules, vol. 82, pp. 273-278, 2016/01/01/ 2016.

[11] S. Adepu and S. Ramakrishna, "Controlled Drug Delivery Systems: Current Status and Future Directions," Molecules, vol. 26, no. 19, p. 5905, 2021.

[12] H. Cortes et al., "Xanthan gum in drug release," Cellular and Molecular Biology, vol. 66, no. 4, pp. 199-207, 2020.

[13] M. Jadav, D. Pooja, D. J. Adams, and H. Kulhari, "Advances in xanthan gum-based systems for the delivery of therapeutic agents," Pharmaceutics, vol. 15, no. 2, p. 402, 2023.

[14] R. Obaidat, A.-S. i. Nizar, T. Bassam, and T. and Athamneh, "Enhancement of levodopa stability when complexed with β-cyclodextrin in transdermal patches," Pharmaceutical Development and Technology, vol. 23, no. 10, pp. 986-997, 2018/11/26 2018.

[15] B. Giordani et al., "Freeze-Dried Matrices Based on Polyanion Polymers for Chlorhexidine Local Release in the Buccal and Vaginal Cavities," Journal of Pharmaceutical Sciences, vol. 108, no. 7, pp. 2447-2457, 2019/07/01/ 2019.

[16] N. M. El-Sawy, A. I. Raafat, N. A. Badawy, and A. M. Mohamed, "Radiation development of pH-responsive (xanthan-acrylic acid)/MgO nanocomposite hydrogels for controlled delivery of methotrexate anticancer drug," International journal of biological macromolecules, vol. 142, pp. 254-264, 2020.

[17] D. Abu Fara et al., "A direct compression matrix made from xanthan gum and low molecular weight chitosan designed to improve compressibility in controlled release tablets," Pharmaceutics, vol. 11, no. 11, p. 603, 2019.

[18] M. Pleguezuelos-Villa et al., "A novel lidocaine hydrochloride mucoadhesive films for periodontal diseases," Journal of Materials Science: Materials in Medicine, vol. 30, no. 1, p. 14, 2019/01/11 2019.

[19] G. O. Akalin and M. Pulat, "Preparation and characterization of nanoporous sodium carboxymethyl cellulose hydrogel beads," Journal of Nanomaterials, vol. 2018, no. 1, p. 9676949, 2018.

[20] X. Wen, D. Bao, M. Chen, A. Zhang, C. Liu, and R. Sun, "Preparation of CMC/HEC crosslinked hydrogels for drug delivery," BioResources, vol. 10, no. 4, pp. 8339-8351, 2015.

[21] A. R. Abbasi et al., "Bioinspired sodium alginate based thermosensitive hydrogel membranes for accelerated wound healing," International journal of biological macromolecules, vol. 155, pp. 751-765, 2020.

[22] G. Sennakesavan, M. Mostakhdemin, L. K. Dkhar, A. Seyfoddin, and S. J. Fatihhi, "Acrylic acid/acrylamide based hydrogels and its properties-A review," Polymer Degradation and Stability, vol. 180, p. 109308, 2020.

[23] M. A. Khan et al., "Synthesis and characterization of acrylamide/acrylic acid Co-polymers and glutaraldehyde crosslinked pH-sensitive hydrogels," Gels, vol. 8, no. 1, p. 47, 2022.

[24] P. P. Dobesh, J. H. J. P. T. J. o. H. P. Oestreich, and D. Therapy, "Ticagrelor: pharmacokinetics, pharmacodynamics, clinical efficacy, and safety," vol. 34, no. 10, pp. 1077-1090, 2014.

[25] S. D. Wiviott and P. G. J. T. L. Steg, "Clinical evidence for oral antiplatelet therapy in acute coronary syndromes," vol. 386, no. 9990, pp. 292-302, 2015.

[26] D. Danielak, M. Karaźniewicz-Łada, and F. J. E. o. o. p. Główka, "Ticagrelor in modern cardiology-an up-to-date review of most important aspects of ticagrelor pharmacotherapy," vol. 19, no. 2, pp. 103-112, 2018.

[27] B. A. Bergmark, N. Mathenge, P. A. Merlini, M. B. Lawrence-Wright, and R. P. J. T. L. Giugliano, "Acute coronary syndromes," vol. 399, no. 10332, pp. 1347-1358, 2022.

[28] R. Teng and J. J. J. o. d. a. Maya, "Absolute bioavailability and regional absorption of ticagrelor in healthy volunteers," vol. 3, no. 1, pp. 43-50, 2014.

[29] M. F. Kabil, A. S. Abo Dena, and I. M. El-Sherbiny, "Chapter Three - Ticagrelor," in Profiles of Drug Substances, Excipients and Related Methodology, vol. 47, A. A. Al-Majed Ed.: Academic Press, 2022, pp. 91-111.

[30] A. Sugidachi, K. Ohno, T. Ogawa, J. Jakubowski, M. Hashimoto, and A. J. B. j. o. p. Tomizawa, "A comparison of the pharmacological profiles of prasugrel and ticagrelor assessed by platelet aggregation, thrombus formation and haemostasis in rats," vol. 169, no. 1, pp. 82-89, 2013.

[31] W. A. Parker and R. F. J. B. Storey, The Journal of the American Society of Hematology, "Ticagrelor: agonising over its mechanisms of action," vol. 128, no. 23, pp. 2595-2597, 2016.

[32] Ticagrelor [Online] Available: https://pubchem.ncbi.nlm.nih.gov/compound/Ticagrelor

[33] M. Akram, I. Taha, and M. M. Ghobashy, "Low temperature pyrolysis of carboxymethylcellulose," Cellulose, vol. 23, no. 3, pp. 1713-1724, 2016/06/01 2016.

[34] I. A. Mohammed and M. M. Ghareeb, "Investigation of Solubility Enhancement Approaches of Ticagrelor," Iraqi Journal of Pharmaceutical Sciences (P-ISSN 1683-3597 E-ISSN 2521-3512), vol. 27, no. 1, pp. 8-19, 2018.

[35] N. C. Sanderson, W. A. Parker, and R. F. J. R. i. C. M. Storey, "Ticagrelor: clinical development and future potential," vol. 22, no. 2, pp. 373-394, 2021.

[36] Ticagrelor. https://www.nhs.uk/medicines/ticagrelor/ (accessed.

[37] D. Danielak, M. Karaźniewicz-Łada, and F. Główka, "Ticagrelor in modern cardiology-an up-to-date review of most important aspects of ticagrelor pharmacotherapy," Expert opinion on pharmacotherapy, vol. 19, no. 2, pp. 103-112, 2018.

[38] B. Huang et al., "Ticagrelor inhibits the NLRP3 inflammasome to protect against inflammatory disease independent of the P2Y12 signaling pathway," vol. 18, no. 5, pp. 1278-1289, 2021.

[39] S. Ahmad, M. Ahmad, K. Manzoor, R. Purwar, and S. Ikram, "A review on latest innovations in natural gums based hydrogels: Preparations & applications," International journal of biological macromolecules, vol. 136, pp. 870-890, 2019.

[40] P. Sánchez-Cid, M. Jiménez-Rosado, A. Romero, and V. Pérez-Puyana, "Novel Trends in Hydrogel Development for Biomedical Applications: A Review," Polymers, vol. 14, no. 15, p. 3023, 2022.

[41] E. Caló and V. V. Khutoryanskiy, "Biomedical applications of hydrogels: A review of patents and commercial products," European Polymer Journal, vol. 65, pp. 252-267, 2015/04/01/ 2015.

[42] J. P. Vareda, A. Lamy-Mendes, and L. Durães, "A reconsideration on the definition of the term aerogel based on current drying trends," Microporous and Mesoporous Materials, vol. 258, pp. 211-216, 2018.

[43] P. Ghasemiyeh and S. Mohammadi-Samani, "Hydrogels as drug delivery systems; pros and cons," Trends in Pharmaceutical Sciences, vol. 5, no. 1, pp. 7-24, 2019.

[44] M. F. Akhtar, M. Hanif, and N. M. Ranjha, "Methods of synthesis of hydrogels... A review," Saudi Pharmaceutical Journal, vol. 24, no. 5, pp. 554-559, 2016.

[45] Z. Man, L. Sidi, Y. Xubo, Z. Jin, and H. Xin, "An in situ catechol functionalized ε-polylysine/polyacrylamide hydrogel formed by hydrogen bonding recombination with high mechanical property for hemostasis," International Journal of Biological Macromolecules, vol. 191, pp. 714-726, 2021.

[46] H. C. Kim, J. N. Lee, E. Kim, M. H. Kim, and W. H. Park, "Self-healable poly (γ-glutamic acid)/chitooligosaccharide hydrogels via ionic and π-interactions," Materials Letters, vol. 297, p. 129987, 2021.

[47] N. Yuan, L. Xu, B. Xu, J. Zhao, and J. Rong, "Chitosan derivative-based self-healable hydrogels with enhanced mechanical properties by high-density dynamic ionic interactions," Carbohydrate polymers, vol. 193, pp. 259-267, 2018.

[48] A. Ullah and S. I. Lim, "Bioinspired tunable hydrogels: An update on methods of preparation, classification, and biomedical and therapeutic applications," International Journal of Pharmaceutics, vol. 612, p. 121368, 2022.

[49] J. Gaar, R. Naffa, and M. Brimble, "Enzymatic and non-enzymatic crosslinks found in collagen and elastin and their chemical synthesis," Organic Chemistry Frontiers, vol. 7, no. 18, pp. 2789-2814, 2020.

[50] A. Wolfel, M. R. Romero, and C. I. A. Igarzabal, "Post-synthesis modification of hydrogels. Total and partial rupture of crosslinks: Formation of aldehyde groups and re-crosslinking of cleaved hydrogels," Polymer, vol. 116, pp. 251-260, 2017.

[51] P. Nezhad-Mokhtari, M. Ghorbani, L. Roshangar, and J. S. Rad, "Chemical gelling of hydrogels-based biological macromolecules for tissue engineering: Photo-and enzymatic-crosslinking methods," International journal of biological macromolecules, vol. 139, pp. 760-772, 2019.

[52] S. Shahi, H. Roghani-Mamaqani, S. Talebi, and H. Mardani, "Stimuli-responsive destructible polymeric hydrogels based on irreversible covalent bond dissociation," Polymer Chemistry, vol. 13, no. 2, pp. 161-192, 2022.

[53] M. A. Campea, M. J. Majcher, A. Lofts, and T. Hoare, "A review of design and fabrication methods for nanoparticle network hydrogels for biomedical, environmental, and industrial applications," Advanced Functional Materials, vol. 31, no. 33, p. 2102355, 2021.

[54] Y. Liu, H. Wei, S. Li, G. Wang, T. Guo, and H. Han, "Facile fabrication of semi-IPN hydrogel adsorbent based on quaternary cellulose via amino-anhydride click reaction in water," International Journal of Biological Macromolecules, vol. 207, pp. 622-634, 2022.

[55] S. Nesrinne and A. Djamel, "Synthesis, characterization and rheological behavior of pH sensitive poly (acrylamide-co-acrylic acid) hydrogels," Arabian Journal of Chemistry, vol. 10, no. 4, pp. 539-547, 2017.

[56] M. C. Koetting, J. T. Peters, S. D. Steichen, and N. A. Peppas, "Stimulus-responsive hydrogels: Theory, modern advances, and applications," Materials Science and Engineering: R: Reports, vol. 93, pp. 1-49, 2015.

[57] S. Zhuo, F. Zhang, J. Yu, X. Zhang, G. Yang, and X. Liu, "pH-Sensitive Biomaterials for Drug Delivery," Molecules, vol. 25, no. 23, p. 5649, 2020.

[58] N. Deirram, C. Zhang, S. S. Kermaniyan, A. P. Johnston, and G. K. Such, "pH-responsive polymer nanoparticles for drug delivery," Macromolecular rapid communications, vol. 40, no. 10, p. 1800917, 2019.

[59] J. Singh and P. Nayak, "pH-responsive polymers for drug delivery: trends and opportunities," Journal of polymer science, vol. 61, no. 22, pp. 2828-2850, 2023.

[60] X. Pang, Y. Jiang, Q. Xiao, A. W. Leung, H. Hua, and C. Xu, "pH-responsive polymer–drug conjugates: design and progress," Journal of controlled release, vol. 222, pp. 116-129, 2016.

[61] J. M. Knipe, F. Chen, and N. A. Peppas, "Enzymatic biodegradation of hydrogels for protein delivery targeted to the small intestine," Biomacromolecules, vol. 16, no. 3, pp. 962-972, 2015.

[62] U. Vegad, M. Patel, D. Khunt, O. Zupančič, S. Chauhan, and A. Paudel, "pH stimuli-responsive hydrogels from non-cellulosic biopolymers for drug delivery," Frontiers in Bioengineering and Biotechnology, vol. 11, p. 1270364, 2023.

[63] A. Hardenia, N. Maheshwari, S. S. Hardenia, S. K. Dwivedi, R. Maheshwari, and R. K. Tekade, "Chapter 1 - Scientific Rationale for Designing Controlled Drug Delivery Systems," in Basic Fundamentals of Drug Delivery, R. K. Tekade Ed.: Academic Press, 2019, pp. 1-28.

[64] P. Gupta, K. Vermani, and S. Garg, "Hydrogels: from controlled release to pH-responsive drug delivery," Drug discovery today, vol. 7, no. 10, pp. 569-579, 2002.

[65] C. Mircioiu et al., "Mathematical Modeling of Release Kinetics from Supramolecular Drug Delivery Systems," Pharmaceutics, vol. 11, no. 3, p. 140, 2019.

[66] K. Park, "Controlled drug delivery systems: Past forward and future back," Journal of Controlled Release, vol. 190, pp. 3-8, 2014/09/28/ 2014.

[67] A. Mahmood, D. Patel, B. Hickson, J. DesRochers, and X. Hu, "Recent progress in biopolymer-based hydrogel materials for biomedical applications," International Journal of Molecular Sciences, vol. 23, no. 3, p. 1415, 2022.

[68] N. A. Pattanashetti, G. B. Heggannavar, and M. Y. Kariduraganavar, "Smart biopolymers and their biomedical applications," Procedia Manufacturing, vol. 12, pp. 263-279, 2017.

[69] M. Rizwan et al., "pH Sensitive Hydrogels in Drug Delivery: Brief History, Properties, Swelling, and Release Mechanism, Material Selection and Applications," Polymers, vol. 9, no. 4, p. 137, 2017.

[70] H. Geckil, X. Feng, Z. Xiaohui, M. SangJun, and U. and Demirci, "Engineering Hydrogels as Extracellular Matrix Mimics," Nanomedicine, vol. 5, no. 3, pp. 469-484, 2010/04/01 2010.

[71] J. Zhu, "Bioactive modification of poly(ethylene glycol) hydrogels for tissue engineering," Biomaterials, vol. 31, no. 17, pp. 4639-4656, 2010/06/01/ 2010.

[72] M. S. B. Reddy, D. Ponnamma, R. Choudhary, and K. K. Sadasivuni, "A comparative review of natural and synthetic biopolymer composite scaffolds," Polymers, vol. 13, no. 7, p. 1105, 2021.

[73] B. Maji and S. Maiti, "Chemical modification of xanthan gum through graft copolymerization: Tailored properties and potential applications in drug delivery and wastewater treatment," Carbohydrate Polymers, vol. 251, p. 117095, 2021/01/01/ 2021.

[74] G. Singhvi, N. Hans, N. Shiva, and S. K. Dubey, "Xanthan gum in drug delivery applications," in Natural polysaccharides in drug delivery and biomedical applications: Elsevier, 2019, pp. 121-144.

[75] A. M. Elgamal, M. H. A. Elella, G. R. Saad, and N. A. Abd El-Ghany, "Synthesis, characterization and swelling behavior of high-performance antimicrobial biocompatible copolymer based on carboxymethyl xanthan," Materials Today Communications, vol. 33, p. 104209, 2022.

[76] P. Kumar, B. Kumar, S. Gihar, and D. Kumar, "Review on emerging trends and challenges in the modification of xanthan gum for various applications," Carbohydrate Research, vol. 538, p. 109070, 2024/04/01/ 2024.

[77] R. Obaidat, N. Al-Shar'i, B. Tashtoush, and T. Athamneh, "Enhancement of levodopa stability when complexed with β-cyclodextrin in transdermal patches," Pharmaceutical development and technology, vol. 23, no. 10, pp. 986-997, 2018.

[78] B. Giordani et al., "Freeze-dried matrices based on polyanion polymers for chlorhexidine local release in the buccal and vaginal cavities," Journal of Pharmaceutical Sciences, vol. 108, no. 7, pp. 2447-2457, 2019.

[79] M. Pleguezuelos-Villa et al., "A novel lidocaine hydrochloride mucoadhesive films for periodontal diseases," Journal of Materials Science: Materials in Medicine, vol. 30, pp. 1-7, 2019.

[80] P. Rakshit, T. K. Giri, and K. Mukherjee, "Research progresses on carboxymethyl xanthan gum: Review of synthesis, physicochemical properties, rheological characterization and applications in drug delivery," International Journal of Biological Macromolecules, p. 131122, 2024.

[81] B. Layek, "A Comprehensive Review of Xanthan Gum-Based Oral Drug Delivery Systems," International Journal of Molecular Sciences, vol. 25, no. 18, p. 10143, 2024.

[82] M. A. S. P. Nur Hazirah, M. I. N. Isa, and N. M. Sarbon, "Effect of xanthan gum on the physical and mechanical properties of gelatin-carboxymethyl cellulose film blends," Food Packaging and Shelf Life, vol. 9, pp. 55-63, 2016/09/01/ 2016.

[83] V. Kanikireddy, K. Varaprasad, T. Jayaramudu, C. Karthikeyan, and R. Sadiku, "Carboxymethyl cellulose-based materials for infection control and wound healing: A review," International Journal of Biological Macromolecules, vol. 164, pp. 963-975, 2020/12/01/ 2020.

[84] N. S. Malik, M. Ahmad, and M. U. Minhas, "Cross-linked β-cyclodextrin and carboxymethyl cellulose hydrogels for controlled drug delivery of acyclovir," PloS one, vol. 12, no. 2, p. e0172727, 2017.

[85] Y. Gupta, M. Sohail Khan, M. Bansal, M. Kumar Singh, K. Pragatheesh, and A. Thakur, "A review of carboxymethyl cellulose composite-based hydrogels in drug delivery applications," Results in Chemistry, vol. 10, p. 101695, 2024/08/01/ 2024.

[86] Y. Hu et al., "A double-layer hydrogel based on alginate-carboxymethyl cellulose and synthetic polymer as sustained drug delivery system," Scientific Reports, vol. 11, no. 1, p. 9142, 2021/04/28 2021.

[87] A. Ashames et al., "Synthesis of cross-linked carboxymethyl cellulose and poly (2-acrylamido-2-methylpropane sulfonic acid) hydrogel for sustained drug release optimized by Box-Behnken Design," Journal of Saudi Chemical Society, vol. 26, no. 6, p. 101541, 2022/11/01/ 2022.

[88] D. Jeong, S.-W. Joo, Y. Hu, V. V. Shinde, E. Cho, and S. Jung, "Carboxymethyl cellulose-based superabsorbent hydrogels containing carboxymehtyl β-cyclodextrin for enhanced mechanical strength and effective drug delivery," European Polymer Journal, vol. 105, pp. 17-25, 2018/08/01/ 2018.

[89] S. M. H. Bukhari, S. Khan, M. Rehanullah, and N. M. Ranjha, "Synthesis and Characterization of Chemically Cross-Linked Acrylic Acid/Gelatin Hydrogels: Effect of pH and Composition on Swelling and Drug Release," International Journal of Polymer Science, vol. 2015, no. 1, p. 187961, 2015.

[90] F. Pervaiz, W. Tanveer, H. Shoukat, and S. Rehman, "Formulation and evaluation of polyethylene glycol/Xanthan gum-co-poly (Acrylic acid) interpenetrating network for controlled release of venlafaxine," Polymer Bulletin, vol. 80, no. 1, pp. 469-493, 2023.

[91] U. Saleem, I. Khalid, L. Hussain, A. Alshammari, and N. A. Albekairi, "Crosslinked PVA-g-poly (AMPS) Nanogels for Enhanced Solubility and Dissolution of Ticagrelor: Synthesis, Characterization, and Toxicity Evaluation," ACS omega, vol. 9, no. 19, pp. 21401-21415, 2024.

[92] A. Aziz et al., "Preparation and Evaluation of a Self-Emulsifying Drug Delivery System for Improving the Solubility and Permeability of Ticagrelor," ACS omega, vol. 9, no. 9, pp. 10522-10538, 2024.

[93] J. PATEL, J. THAKOR, D. PATEL, V. PATEL, S. PARIKH, and R. PATEL, "FORMULATION AND EVALUATION OF SUSTAINED RELEASE TABLETS OF TICAGRELOR."

[94] U. Shastri, K. P. Sutar, V. A. Jadhav, and N. S. Shirkoli, "Formulation, optimization and evaluation of ticagrelor liquisolid tablets for enhanced solubility," Research Journal of Pharmacy and Technology, vol. 17, no. 4, pp. 1453-1460, 2024.

[95] Z. F. Alsafar, M. S. Al_lami, and Z. Haroon, "Formulation, Characterization, and Evaluation of Ticagrelor-loaded Nano Micelles Enhance Intestinal Absorption," Bahrain Medical Bulletin, vol. 45, no. 2, 2023.

[96] Alsaad, A. A, "Solubility Enhancement of Ticagrelor by Different Complexation Methods," Journal for Reattach Therapy and Developmental Diversities, vol , pp. 494-505, 2022.

[97] N. Shahid et al., "Synthesis and evaluation of chitosan based controlled release nanoparticles for the delivery of ticagrelor," Designed monomers and polymers, vol. 25, no. 1, pp. 55-63, 2022.

[98] K. W. Khalid and S. N. Abd Alhammid, "Preparation and in-vivo Evaluation of Ticagrelor Oral Liquid Self nano-emulsion," J. Pharm. Negat. Results, vol. 13, no. 3, p. 274, 2022.

[99] N. Shahid et al., "Fabrication of thiolated chitosan based biodegradable nanoparticles of ticagrelor and their pharmacokinetics," Polymers and Polymer Composites, vol. 30, p. 09673911221108742, 2022.

[100] R. S. Vadapalli and M. Sunitha Reddy, "Formulation and Evaluation of Self-Micro Emulsifying Drug Delivery System (SMEDDS) of Ticagrelor," Saudi J Med Pharm Sci, vol. 8, no. 11, pp. 628-643, 2022.

[101] N. Hosseini-Ashtiani and A. Tadjarodi, "Design and Characterization of Ticagrelor-Loaded Chitosan Biopolymer to Improve Chemical and Biological Properties of the Drug," ChemistrySelect, vol. 6, no. 8, pp. 1741-1747, 2021.

[102] L. Hao et al., "Preparation and in vivo/in vitro characterization of Ticagrelor PLGA sustained-release microspheres for injection," Designed Monomers and Polymers, vol. 24, no. 1, pp. 305-319, 2021.

[103] N. Shahid et al., "pH-Responsive nanocomposite based hydrogels for the controlled delivery of ticagrelor; in vitro and in vivo approaches," International Journal of Nanomedicine, pp. 6345-6366, 2021.

[104] M. Zaman et al., "Synthesis of thiol-modified hemicellulose, its biocompatibility, studies, and appraisal as a sustained release carrier of ticagrelor," Frontiers in Pharmacology, vol. 12, p. 550020, 2021.

[105] M. Yadav, J. Sarolia, B. Vyas, M. Lalan, S. Mangrulkar, and P. Shah, "Amalgamation of solid dispersion and melt adsorption technique: improved in vitro and in vivo performance of ticagrelor tablets," AAPS PharmSciTech, vol. 22, pp. 1-21, 2021.

[106] Y.-G. Na et al., "Development and evaluation of TPGS/PVA-based nanosuspension for enhancing dissolution and oral bioavailability of ticagrelor," International Journal of Pharmaceutics, vol. 581, p. 119287, 2020.

[107] M. Zaman, R. I. Bajwa, S. Saeed, M. A. Hussain, and M. Hanif, "Synthesis and characterization of thiol modified beta cyclodextrin, its biocompatible analysis and application as a modified release carrier of ticagrelor," Biomedical Materials, vol. 16, no. 1, p. 015023, 2020.

[108] I. A. Mohammed and M. M. Ghareeb, "Investigation of solubility enhancement approaches of ticagrelor," Iraqi Journal of Pharmaceutical Sciences, vol. 27, no. 1, pp. 8-19, 2018.

[109] H. Shoukat et al., "Development of β-cyclodextrin/polyvinypyrrolidone-co-poly (2-acrylamide-2-methylpropane sulphonic acid) hybrid nanogels as nanodrug delivery carriers to enhance the solubility of Rosuvastatin: An in vitro and in vivo evaluation," Plos one, vol. 17, no. 1, p. e0263026, 2022.

[110] Y. Wang et al., "Chitosan cross-linked poly (acrylic acid) hydrogels: Drug release control and mechanism," Colloids and Surfaces B: Biointerfaces, vol. 152, pp. 252-259, 2017.

[111] A. Salawi et al., "Development of Statistically Optimized Chemically Cross-Linked Hydrogel for the Sustained-Release Delivery of Favipiravir," Polymers, vol. 14, no. 12, p. 2369, 2022.

[112] J. Mudassir, A. K. Sherwani, A. Hussain, N. Abbas, and M. S. Arshad, "Formulation, Optimization and Characterization of Chitosan Monodisperse

Microparticles for Sustained Delivery of Hydrochlorothiazide HCl," Pharmaceutical Sciences, vol. 26, no. 3, pp. 306-313, 2020.

[113] K. Dharmalingam and R. Anandalakshmi, "Fabrication, characterization and drug loading efficiency of citric acid crosslinked NaCMC-HPMC hydrogel films for wound healing drug delivery applications," International journal of biological macromolecules, vol. 134, pp. 815-829, 2019.

[114] K. Sohail, I. U. Khan, Y. Shahzad, T. Hussain, and N. M. Ranjha, "pH-sensitive polyvinylpyrrolidone-acrylic acid hydrogels: Impact of material parameters on swelling and drug release," Brazilian Journal of Pharmaceutical Sciences, vol. 50, no. 1, pp. 173-184, 2014.

[115] T. Mahmood et al., "Preparation, In Vitro Characterization, and Evaluation of Polymeric pH-Responsive Hydrogels for Controlled Drug Release," ACS omega, vol. 9, no. 9, pp. 10498-10516, 2024.

[116] R. M. Sarfraz et al., "Development and In-Vitro Evaluation of pH Responsive Polymeric Nano Hydrogel Carrier System for Gastro-Protective Delivery of Naproxen Sodium," Advances in Polymer Technology, vol. 2019, no. 1, p. 6090965, 2019.

[117] M. Rezvanian, N. Ahmad, M. C. I. M. Amin, and S.-F. Ng, "Optimization, characterization, and in vitro assessment of alginate-pectin ionic cross-linked hydrogel film for wound dressing applications," International journal of biological macromolecules, vol. 97, pp. 131-140, 2017.

[118] U. G. T. M. Sampath, Y. C. Ching, C. H. Chuah, R. Singh, and P.-C. Lin, "Preparation and characterization of nanocellulose reinforced semi-interpenetrating polymer network of chitosan hydrogel," Cellulose, vol. 24, no. 5, pp. 2215-2228, 2017/05/01 2017.

[119] P. Sarika, P. A. Kumar, D. K. Raj, and N. R. James, "Nanogels based on alginic aldehyde and gelatin by inverse miniemulsion technique: synthesis and characterization," Carbohydrate polymers, vol. 119, pp. 118-125, 2015.

[120] X. L. Ni et al., "In vitro and in vivo antitumor effect of gefitinib nanoparticles on human lung cancer," Drug delivery, vol. 24, no. 1, pp. 1501-1512, 2017.

[121] A. Mahmood et al., "Development and Evaluation of Sodium Alginate/Carbopol 934P-Co-Poly (Methacrylate) Hydrogels for Localized Drug Delivery," Polymers, vol. 15, no. 2, p. 311, 2023.

[122] M. Suhail et al., "Xanthan-Gum/Pluronic-F-127-Based-Drug-Loaded Polymeric Hydrogels Synthesized by Free Radical Polymerization Technique for Management of Attention-Deficit/Hyperactivity Disorder," Gels, vol. 9, no. 8, p. 640, 2023.

[123] R. M. Sarfraz et al., "Synthesis of co-polymeric network of carbopol-g-methacrylic acid nanogels drug carrier system for gastro-protective delivery of ketoprofen and its evaluation," Polymer-Plastics Technology and Materials, vol. 59, no. 10, pp. 1109-1123, 2020.

[124] N. Ranjha, M. A. Madni, A. Bakar, N. Talib, S. Ahmad, and H. Ahmad, "Preparation and Characterization of Isosorbide Mononitrate Hydrogels Obtained by Free-Radical Polymerization for Site-Specific Delivery," Tropical Journal of Pharmaceutical Research, vol. 13, pp. 1979-85, 12/15 2014.

[125] S. S. Bhattacharya et al., "Synthesis and Characterization of Poly(acrylic acid)/Poly(vinyl alcohol)-xanthan Gum Interpenetrating Network (IPN) Superabsorbent Polymeric Composites," Polymer-Plastics Technology and Engineering, vol. 51, no. 9, pp. 878-884, 2012/06/01 2012.

[126] N. S. Malik, M. Ahmad, M. U. Minhas, G. Murtaza, and Q. Khalid, "Polysaccharide hydrogels for controlled release of acyclovir: development, characterization and in vitro evaluation studies," Polymer Bulletin, vol. 74, pp. 4311-4328, 2017.

[127] H. Ijaz, U. R. Tulain, and J. Qureshi, "Formulation and In-vitro Evaluation of pH Sensitive Crosslinked Xanthan Gum Grafted-Acrylic Acid Copolymer for Controlled Delivery of Perindopril Erbumine (PE)," Polymer-Plastics Technology and Engineering, 11/17 2017.

[128] A. A. Umaredkar, P. V. Dangre, D. K. Mahapatra, and D. M. Dhabarde, "Fabrication of chitosan-alginate polyelectrolyte complexed hydrogel for controlled release of cilnidipine: A statistical design approach," Materials Technology, vol. 35, no. 11-12, pp. 697-707, 2020.

[129] Tushar, Y. Saraswat, P. Meena, and S. G. Warkar, "Synthesis and characterization of novel xanthan gum-based pH-sensitive hydrogel for metformin hydrochloride release," Colloid and Polymer Science, vol. 301, no. 10, pp. 1147-1158, 2023/10/01 2023.

[130] N. S. Malik et al., "Chitosan/Xanthan Gum Based Hydrogels as Potential Carrier for an Antiviral Drug: Fabrication, Characterization, and Safety Evaluation," (in English), Frontiers in Chemistry, Original Research vol. 8, 2020-February-04 2020.

[131] F. Al-Akayleh, M. Al-Remawi, M. Salem, and A. Badwan, "Using chitosan and xanthan gum mixtures as excipients in controlled release formulations of ambroxol HCl - in vitro drug release and swelling behavior," Journal of Excipients and Food Chemicals, vol. 5, pp. 140-148, 06/01 2014.

[132] V. B. Bueno and D. F. S. Petri, "Xanthan hydrogel films: Molecular conformation, charge density and protein carriers," Carbohydrate Polymers, vol. 101, pp. 897-904, 2014/01/30/ 2014.

[133] N. F. Che Nan, N. Zainuddin, and M. Ahmad, "Preparation and Swelling Study of CMC Hydrogel as Potential Superabsorbent," Pertanika Journal of Science & Technology, vol. 27, no. 1, 2019.

[134] M. C. I. Mohd Amin, N. Ahmad, M. Pandey, and C. Jue Xin, "Stimuli-responsive bacterial cellulose-g-poly (acrylic acid-co-acrylamide) hydrogels for oral controlled release drug delivery," Drug development and industrial pharmacy, vol. 40, no. 10, pp. 1340-1349, 2014.

[135] H. Ijaz et al., "Design and in vitro evaluation of pH-sensitive crosslinked chitosan-grafted acrylic acid copolymer (CS-co-AA) for targeted drug delivery," International Journal of Polymeric Materials and Polymeric Biomaterials, vol. 71, no. 5, pp. 336-348, 2022.

[136] M. Rizky and N. M. Nizardo, "The effect of monomer ratio and crosslinker concentration on swelling behavior of pH-responsive poly(hydroxymethyl acrylamide-co-acrylamide)," AIP Conference Proceedings, vol. 2374, no. 1, 2021.

[137] P. Meena, P. Singh, and S. G. Warkar, "Fabrication and evaluation of stimuli-sensitive xanthan gum-based hydrogel as a potential carrier for a hydrophobic drug ibuprofen," Colloid and Polymer Science, vol. 302, no. 3, pp. 377-391, 2024.

[138] S. Sethi, Saruchi, B. S. Kaith, M. Kaur, N. Sharma, and V. Kumar, "Crosslinked xanthan gum–starch hydrogels as promising materials for controlled drug delivery," Cellulose, vol. 27, pp. 4565-4589, 2020.

[139] N. Shahid et al., "Fabrication of thiolated chitosan based biodegradable nanoparticles of ticagrelor and their pharmacokinetics," Polymers and Polymer Composites, vol. 30, p. 09673911221108742, 2022.

[140] M. C. I. M. Amin, N. Ahmad, N. Halib, and I. Ahmad, "Synthesis and characterization of thermo-and pH-responsive bacterial cellulose/acrylic acid hydrogels for drug delivery," Carbohydrate Polymers, vol. 88, no. 2, pp. 465-473, 2012.

[141] T. Riaz et al., "FTIR analysis of natural and synthetic collagen," Applied Spectroscopy Reviews, vol. 53, no. 9, pp. 703-746, 2018.

[142] N. S. Malik et al., "Chitosan/xanthan gum based hydrogels as potential carrier for an antiviral drug: Fabrication, characterization, and safety evaluation," Frontiers in chemistry, vol. 8, p. 50, 2020.

[143] A. Meas, E. Wi, M. Chang, and H. S. Hwang, "Carboxylmethyl cellulose produced from wood sawdust for improving properties of sodium alginate

hydrogel in dye adsorption," Separation and Purification Technology, vol. 341, p. 126906, 2024.

[144] M. Anwar et al., "Formulation and evaluation of interpenetrating network of xanthan gum and polyvinylpyrrolidone as a hydrophilic matrix for controlled drug delivery system," Polymer Bulletin, vol. 78, pp. 59-80, 2021.

[145] S. Sethi, Saruchi, B. S. Kaith, M. Kaur, N. Sharma, and V. Kumar, "Cross-linked xanthan gum–starch hydrogels as promising materials for controlled drug delivery," Cellulose, vol. 27, no. 8, pp. 4565-4589, 2020/05/01 2020.

[146] U. Saleem, I. Khalid, L. Hussain, A. Alshammari, and N. A. Albekairi, "Crosslinked PVA-g-poly(AMPS) Nanogels for Enhanced Solubility and Dissolution of Ticagrelor: Synthesis, Characterization, and Toxicity Evaluation," ACS Omega, vol. 9, no. 19, pp. 21401-21415, 2024/05/14 2024.

[147] S. Thomas, P. Soloman, and V. Rejini, "Preparation of chitosan-CMC blends and studies on thermal properties," Procedia Technology, vol. 24, pp. 721-726, 2016.

[148] S. D. Yuwono, E. Wahyuningsih, A. A. Noviany, W. Simanjuntak, and S. Hadi, "Characterization of carboxymethyl cellulose (CMC) synthesized from microcellulose of cassava peel," Mater. Plast, vol. 57, no. 4, pp. 225-235, 2021.

[149] A. Ashames et al., "Development, characterization and In-vitro evaluation of guar gum based new polymeric matrices for controlled delivery using metformin HCl as model drug," PLoS One, vol. 17, no. 7, p. e0271623, 2022.

[150] S. A. Murtale et al., "Synthesis and evaluation of grafted xanthan gum as a drug carrier in developing lornoxicam gel formulations," Pharmacognosy Magazine, vol. 18, no. 80, 2022.

[151] N. Batool et al., "Development and evaluation of cellulose derivative and pectin based swellable pH responsive hydrogel network for controlled delivery of cytarabine," Gels, vol. 9, no. 1, p. 60, 2023.

[152] G. Pai and M. B. Sathyanarayana, "Fabrication and solid state characterization of ticagrelor co-crystals with improved solubility and dissolution," BDL, vol. 20, no. 14.54, pp. 13-98, 2017.

[153] A. M. Heimbuck, T. R. Priddy-Arrington, B. J. Sawyer, and M. E. Caldorera-Moore, "Effects of post-processing methods on chitosan-genipin hydrogel properties," Materials Science and Engineering: C, vol. 98, pp. 612-618, 2019/05/01/ 2019.

[154] S. Durkut, "Thermoresponsive poly (N-vinylcaprolactam)-g-galactosylated chitosan hydrogel: Synthesis, characterization, and controlled release properties," International Journal of Polymeric Materials and Polymeric Biomaterials, vol. 68, no. 17, pp. 1034-1047, 2019.

[155] G.-F. Wang, H.-J. Chu, H.-L. Wei, X.-Q. Liu, Z.-X. Zhao, and J. Zhu, "Click synthesis by Diels-Alder reaction and characterisation of hydroxypropyl methylcellulose-based hydrogels," Chemical Papers, vol. 68, no. 10, pp. 1390-1399, 2014/10/01 2014.

[156] Q. Khalid, M. Ahmad, M. U. Minhas, F. Batool, N. S. Malik, and M. Rehman, "Novel β-cyclodextrin nanosponges by chain growth condensation for solubility enhancement of dexibuprofen: Characterization and acute oral toxicity studies," Journal of Drug Delivery Science and Technology, vol. 61, p. 102089, 2021.

[157] O. Abdullah, M. Usman Minhas, M. Ahmad, S. Ahmad, K. Barkat, and A. Ahmad, "Synthesis, optimization, and evaluation of polyvinyl alcohol-based hydrogels as controlled combinatorial drug delivery system for colon cancer," Advances in Polymer Technology, vol. 37, no. 8, pp. 3348-3363, 2018.